Triple-axis neutron-scattering study of phason dynamics in Al-Mn-Pd quasicrystals

Gerrit Coddens,* Sandrine Lyonnard,† and Bernard Hennion
Laboratoire Léon Brillouin, CEA/CNRS, F-91191-Gif-sur-Yvette CEDEX, France

Yvonne Calvayrac
CECM/CNRS, F-94407-Vitry CEDEX, France

(Received 10 May 1999)

We present an extensive triple-axis neutron-scattering study of phason hopping in a single-domain sample of a perfect icosahedral $Al_{70.4}Mn_{8.6}Pd_{21.0}$ quasicrystal. The quasielastic intensities exhibit important anisotropies. They are compared with models at various levels of sophistication. This comparison strongly suggests the occurrence of *simultaneous correlated* jumps. The important correlations are directed along the threefold axes.

I. INTRODUCTION: PHASON DYNAMICS

Phason dynamics[1–10] plays a key part in the understanding of many basic structural and dynamical properties of quasicrystals (QCs), and have been extensively studied during the last years, both experimentally and theoretically. The terminology phason was coined by analogy with incommensurate phases,[12,13] but is *a priori* a misnomer that has to be handled with circumspection: Although incommensurate crystals and QCs belong to the same family of quasiperiodic structures, their topological properties are very different.[14] In the cut-and-projection method, a quasiperiodic structure is obtained by embedding it into a superspace of higher dimension, wherein a periodic lattice has been defined. Each intersection between the ''atomic surfaces'' decorating this high-dimensional periodic lattice and the physical space yields one atomic position.[16] Incommensurate crystals are obtained from large continuous components, while it has been shown that atomic surfaces are generally *not* continuous in QCs. Consequently, a *global* rigid translation of the cut parallel to itself generates propagating modes (so-called phason modes) (Ref. 17) in incommensurate crystals, while only *local* deformations leading to *discrete atomic jumps* are expected to occur in QCs. That such jumps are now dubbed ''phasons'' stems from a historical clumsiness, since the word ''phason'' irresistibly conjures up a wrong image of continuous collective modes of atomic motion. This important remark can almost serve as a definition,[15] viz., that one of the hallmarks of a QC is that it is a *quasiperiodic object whose phasons are not propagating modes*.

In view of the importance of phason dynamics for a variety of theoretical issues to be briefly underlined below, and which encompass structure, growth, stability, diffusion processes, and phase transitions of QCs, we have undertaken a systematic investigation of atomic hopping. We are relating here the results of a series of triple-axis experiments by quasielastic neutron scattering on a single-grain Al-Mn-Pd QC.

Phason dynamics is endowed with an important role in theories dealing with the thermodynamical stability of the structure of QCs. Whatever the option choosen to study stabilization processes, the existence of atomic jumps is a critical assertion. In the random-tiling model,[18] the existence of a crystalline ground state is postulated. It is this phase that is stable at low temperatures. With increasing temperature, the number of phason flips considerably increases and leads to a transition to a random QC state. The transition is driven by the very high configurational entropy that can result from the tile flips. A random tiling is thus obtained from a perfect QC by applying a succession of elementary phason flips which do not destroy the long-range quasiperiodic order. On the other hand, in the model of perfect QCs,[19] the fundamental state of the structure (minimizing the free energy) is the QC state. Real QCs appear as the unperfect realization of this state, and phason defects exist in the structure as naturally as chemical disorder or vacancies in a crystal. To explain the existence of such perfect QCs, a special self-diffusion mechanism based on phason jumps has been proposed by Kalugin and Katz.[20] In fact, there are no local growth rules for a number of Penrose tilings, which are the core of all conceptual tools on which our comprehension of QCs has been founded.[21] One then starts to wonder how they can grow to such a high perfection.[22] According to the random-tiling model the answer is that they do contain a lot of disorder.[23] Within the model of the perfect QC, defects produced during the growth are rapidly annealed out due to the fast diffusion. Within the model of Kalugin and Katz long-range diffusion can be generated by a domino sequence of a large number of local tile reshuffles. A percolation regime could be reached at high temperatures and lead to an unusual acceleration of the diffusion, deviating from the standard Arrhenius behavior that is traditionally observed in metallic alloys. Phason-driven diffusion is predicted to dominate in QCs, but the theory does not quantify the relevant temperature range. Moreover, the model stipulates a very low activation energy for individual phason jumps, and a possible transition between a perfect QC and a randomized tiling.[24–26] Several aspects of this theory were reproduced in computer simulations.[27–30] However, a steadily increasing body of macroscopic measurements[31–37] of diffusion coefficients in QCs by tracer methods consistently fails to show any sign of accelerated diffusion below the melting temperature. This outcome remains the bogey riddle for the theory of Kalugin and Katz *sensu stricto*.[21] In this context, a specific study of

the phason jumps is of interest to document the properties of self-diffusion in QCs.

The existence of two different epistemologies for QCs—the random-tiling model and the perfect-QC model—is not only rooted in our ignorance with respect to the growth mechanisms, but also an offshoot of the difficulties encountered in giving a complete structural description of these materials. The QC structure is globally well described by six-dimensional (6D) quasicrystallography, but an uncertainty remains concerning the Bragg peaks of weak intensities which in principle should code the fine details of the atomic structure. To summarize the situation: the very high degree of perfection of last-generation icosahedral QCs remains partially mysterious, and the problem of unraveling the exact positions of all atoms is still not solved. Admitting we can reach the experimental accuracy required, the determination of jump parameters (such as vectors and atomic species involved) could shed some light on the structural problem[19,38,39] by providing crucial tests of the interatomic distances and spatial distributions.

A number of phase transitions[24–26] and mechanical properties of QCs have also been related to phason jumps. This fact constitutes a motivation to understand the elementary jump processes. First of all, the thermal activation of phason jumps could intervene in phase transitions between QCs and periodic approximants,[40–43] as the key move in the atomic rearrangements that allow one to pass from one structure to another. The mechanisms leading to the formation of metastable intermediary states most probably also involve modifications of the local structure of the materials that are phason driven. Another possible case in point is the brittle-ductile transition[44] observed at high temperature.[45] The plastic properties of QCs are drastically modified on increasing the temperature: whereas QCs are very hard and brittle at room temperature, they behave like remarkably superplastic materials at high temperatures. Phason-based scenarios have been proposed as a rationale that could account for these amazing properties, but they have not yet been validated. Finally, one has also invoked phason-based scenarios to come to grips with some mechanical properties of QCs, manifested, e.g., in vibrating-reed experiments.[46]

Some very preliminary results of this project have been reported in conference proceedings[7] and in a thesis.[47] They are partly superseded by the aforelying presentation. In a first, introductory part of the article (Sec. II), we justify the scope of the present triple-axis study by putting it into a technical perspective. From this we will learn what kind of results will be the unique resort of this type of study and what sorts of questions are better tackled by other experimental methods. Also a short description of the basic jump model is recalled. In Sec. III we briefly review an anthology of previous results. We will single out just those aspects that are necessary to provide the reader with some appropriate background information. In Sec. IV we start to develop our experimental line of approach by scouting surveys on two fronts: We try to gain some insights from a few simple model calculations and from the results of a reconnaissance time-of-flight (TOF) experiment. In Sec. V we give the protocol of the triple-axis experiments. In Sec. VI we give a detailed account of the data analysis, while in the next section we present the experimental results. Section VIII is devoted to the confrontation of these results with a number of models. Finally, we conclude in Sec. IX.

II. TECHNICAL PREAMBLE

A. Experimental technique: Quasielastic neutron scattering

Only a few techniques are actually available to observe and study atomic jumps: Mössbauer spectroscopy,[2–4] nuclear magnetic resonance,[48,49] and quasielastic neutron scattering. We mainly performed neutron-scattering experiments,[1,5,6] completed by some additional ^{57}Fe Mössbauer measurements.[2] Thermal (or cold) neutrons have energies of the order of magnitude of the vibrational motion in solids, and constitute therefore the tool of excellence for our kind of study.

The scattering function $S(\mathbf{Q},\omega)$ that is measured is the Fourier transform of spatio-temporal Van Hove[50] correlation functions $G(\mathbf{r},t)$ between particles,[51,52] where $\mathbf{Q}=\mathbf{k}_i-\mathbf{k}_f$ is the momentum transfer and $\hbar\omega=E_i-E_f$ the energy transfer of the neutron. The Van Hove *total (self-)*correlation functions are giving the probability to find a particle at position $\mathbf{r}$ and instant t if *any (the same)* particle was situated at position vector $\mathbf{0}$ at instant 0. They correspond to the *total (incoherent)* scattering functions. Atomic jumps are dynamical processes implying small energy transfers which are accessible by quasielastic neutron scattering. The hopping distances amount to 1–2 interatomic distances, typically a few Å in icosahedral QCs. Consequently the useful range in reciprocal space to study jump signals extends well up to $|\mathbf{Q}|=5$ Å^{-1}. A number of models of various degrees of complication and sophistication can be used to analyze hopping signals (as will be discussed later), but the canonical one—featuring the jump of a single atom in a double-well potential—has been successfully applied to analyze all our previous data.[51,52] Since there is only one particle, the distinction between total and incoherent scattering functions ceases to exist within this model. Considering two equivalent sites separated by a jump vector $\mathbf{d}$ and a relaxation time τ, the scattering function is given by

$$S(\mathbf{Q},\omega)=\frac{1}{2}[1+\cos(\mathbf{Q}\cdot\mathbf{d})]\,\delta(\omega)+\frac{1}{2}[1-\cos(\mathbf{Q}\cdot\mathbf{d})]\frac{1}{\pi}\frac{\Gamma}{\Gamma^2+(\hbar\omega)^2}. \quad (1)$$

The first term is a Dirac peak positioned at zero-energy transfer, the intensity of which is modulated by the so-called (incoherent) elastic structure factor. It corresponds to the static contribution of the system, i.e., to the probability that an atom stays in a same site. The second term is also centered on zero-energy transfer and is the quasielastic Lorentzian-shaped contribution arising from the dynamical jump process. Its half width at half maximum Γ is inversely proportional to the relaxation time of the jump: the wider the signal, the quicker the jump. Its intensity is modulated by the quasielastic form factor which is the spatial Fourier transform of the dipole produced by putting a Dirac measure in both minima of the double well and depends on the jump vector $\mathbf{d}$. It may be noted that the quasielastic structure factor and the elastic structure factor[53] obey *a sum rule*: their sum is a

TABLE I. Neutron-scattering cross sections.

Isotope	$\sigma_{inc}(b)$	$\sigma_{coh}(b)$
^{27}Al	-	1.495
^{57}Fe	0.5	0.66
^{54}Fe	-	2.2
^{nat}Fe	0.39	11.44
^{63}Cu	6×10^{-3}	5.52
^{65}Cu	0.4	14.1
^{nat}Cu	0.52	7.49
^{55}Mn	0.6	1.65
^{105}Pd	-	4.1
^{106}Pd	-	3.8
^{108}Pd	-	2.11
^{nat}Pd	0.09	4.1

constant, viz., 1, such that the **Q** dependence of one of them is the opposite of the **Q** dependence of the other one. Both contributions are in practice attenuated by the Debye-Waller factor and convoluted with the experimental resolution function. In the case of single-grain QCs, where the signal can be studied as a function of the momentum transfer vector **Q**, the full content of the geometrical information thus lies open for study: the distance *and* the orientation of the jump can be simultaneously obtained. In the case of powder samples (with no texture), an average over the isotropic distribution of all possible grain orientations yields the quasielastic structure factor $F_{powder}(\mathbf{Q})=\frac{1}{2}[1-j_0(Qd)]$, which only depends on the jump distance. The information on jump orientation, which would be a critical parameter, e.g., to cross-check structural models, is then lost. This remark highlights the importance of a triple-axis study on a single-grain sample.

B. Al-Cu-Fe and Al-Mn-Pd quasicrystals

The first QCs were strongly disordered, exhibiting an important broadening of the Bragg peaks which rendered them of moderate interest for accurate studies. Nowadays, a new generation[54–58] of almost perfect[22] icosahedral phases has become available. X-ray patterns from Al-Cu-Fe and Al-Mn-Pd systems exhibit sharp Bragg peaks, the widths of which are resolution limited. Such QCs are ideal systems for the study of atomic jumps.[59] The atomic structures of Al-Mn-Pd and Al-Cu-Fe are rather similar, with atoms of Fe playing the same part in Al-Cu-Fe as atoms of Mn in Al-Mn-Pd, and atoms of Cu the same role as atoms of Pd. However, even if both phases are equally perfect and comparable from the structural point of view, they offer quite different technical possibilities.

(1) *Neutron-scattering lengths*. One of the unique advantages of neutron scattering is that it allows one to exploit strong constrasts that may arise between scattering lengths of different isotopes of the same chemical species. For instance the contrast between the hydrogen and deuterium cross sections has been profusively put to profit in studies of organic systems in soft condensed matter.[60] Table I lists the values of the incoherent and coherent neutron-scattering cross sections for Al, Cu, Fe, Mn, and Pd.[61] We may note that all these elements have a negligible incoherent contribution, such that the signals collected in the experiments will predominantly arise from coherent scattering. The Al cross section is very low, and it is therefore almost impossible to observe Al dynamics by the neutron-scattering technique. This is all the more disappointing as Al makes up for roughly 70% of our QCs. A strong contrast does exist between ^{nat}Cu, ^{63}Cu, and ^{65}Cu, as well as between ^{nat}Fe, ^{54}Fe, and ^{57}Fe. For example, Cu dynamics in a sample fully enriched in ^{65}Cu will show up with an intensity that is twice as strong as in a sample prepared from ^{nat}Cu. Similarly, a sample with ^{nat}Fe will enhance the signal from Fe dynamics by a factor of 5 with respect to a comparable sample based on ^{54}Fe. Such contrasts render isotopic studies possible and very interesting in Al-Cu-Fe: Cu dynamics on the one hand and Fe dynamics on the other can be very well distinguished. The prospects for squeezing out the same kind of detailed information from the Al-Mn-Pd system are looking dim: as Al, Mn is monoisotopic, and the contrast between the various Pd isotopes is not sufficient. A substitution of ^{nat}Pd by ^{108}Pd could be useful, but the prohibitive cost of isotopic enrichment rules out the feasibility of such a study. In conclusion isotopic substitution is out of the question within the Al-Mn-Pd system, and no direct information about the atomic species participating in the jumps can be gained from neutron-scattering experiments. A first possibility one can think of to overcome this drawback would be to check if there exist alternative techniques that are sensitive to a given element, such as ^{57}Fe Mössbauer spectroscopy to single out the Fe dynamics or NMR to investigate Al relaxation within the system. But Pd and Mn do not offer such possibilities. The second angle of approach consists in the ''poor man's'' method of comparing systematically the Al-Mn-Pd experimental results to those obtained in Al-Cu-Fe and making the structural analogy between the two icosahedral phases. We have used this method frequently as a basis for formulating educated guesses about the identification of the Mn and Pd jumps. Nevertheless, in order to remind ourselves that such a tentative attribution of a chemical species to a jump can only take on the status of a weak presumption, we will adopt throughout the article a notation between parentheses: (Mn), (Pd), and (Al).

(2) *Phase diagrams*. The second important difference between Al-Cu-Fe and Al-Mn-Pd systems resides in the possibility or otherwise of growing single-grain samples that are large enough for neutron-scattering measurements, which require volumes of a few cm^3. Both the Al-Cu-Fe and the Al-Mn-Pd phase diagrams are rather intricate,[62,63] and the stability domains of the icosahedral phases are slender. In the case of Al-Cu-Fe, the icosahedral region is not connected to the liquidus, such that it is impossible to grow a cm-sized single-grain QC under equilibrium conditions with the right stoichiometric composition from the melt. Millimeter-sized samples can be obtained, useful for instance to make Mössbauer[64] studies at dedicated beam lines of third-generation synchrotron sources, where the high brilliance and the reduced beam size enable one to study the scattering from tiny samples. But neutron triple-axis experiments are not feasible with such small QCs. Lograsso and Delaney[56] have produced large single grains of Al-Cu-Fe, but they are of lesser structural quality. Fortunately, in the case of Al-Mn-Pd it is possible to grow large single grains from the

TABLE II. Summary of atomic-hopping results.

Sample	Γ (μeV)	Atom	E_a (meV)	d(Å)	Axis	References
i-$Al_{62}Cu_{25.5}Fe_{12.5}$	2.5/4	Fe	-	-	-	2,4,5[a,b]
i-$Al_{62}Cu_{25.5}Fe_{12.5}$	55	Cu	750	3.9	-	1[c]
i-$Al_{62}Cu_{25.5}Fe_{12.5}$	250	Cu	450	$\leqslant 2$	-	1[c]
i-$Al_{62}Cu_{25.5}Fe_{12.5}$	900	All	-	-	-	1[c]
β-$Al_{50}Cu_{25}Fe_{25}$	-	None	-	-	-	1[c]
i-$Al_{62.5}Cu_{26.5}Fe_{11}$	64 ± 35	(Cu)	-	-	-	5[c,d]
r-$Al_{62.5}Cu_{26.5}Fe_{11}$	64 ± 35	(Cu)	-	-	-	5[c,d]
α-$Al_{55}Si_7Cu_{25.5}Fe_{12.5}$	-	None	-	-	-	5[c]
i-$Al_{70.3}Mn_{8.3}Pd_{21.4}$	2.5	(Mn)	-	-	-	6[b]
i-$Al_{70.3}Mn_{8.3}Pd_{21.4}$	200	(Pd)	270	?	?	6[c,e]
i-$Al_{70.3}Mn_{8.3}Pd_{21.4}$	400	(Pd)	170	3.8	3	6[c,e]
i-$Al_{70.3}Mn_{8.3}Pd_{21.4}$	400	?	170	?	3	6[c,e]
d-$Al_{71}Co_{12}Ni_{17}$	365	Not Ni	553	$\leqslant 2$	-	8[c]
d-$Al_{71}Co_{12}Ni_{17}$	150	Ni	-	-	-	8[c]
$Ti_{45}Ni_{17}Zr_{38}H_{150}$	140	H	130	$\leqslant 2$	-	70,71[c,f]
$Ti_{45}Ni_{17}Zr_{38}D_{160}$	140	D	92	$\leqslant 2$	-	71[f,g]

[a]Mössbauer spectroscopy.
[b]Neutron backscattering (IN16).
[c]Neutron time of flight (MIBEMOL).
[d]This sample was obtained once in the rhombohedral and once in the icosahedral phase.
[e]Neutron triple axis (4F2).
[f]Neutron time of flight (TFXA).
[g]Neutron time of flight (IN6).

liquidus by drawing methods. For this alloy the determination of jump vectors on a triple-axis spectrometer is thus no longer impossible.

(3) *Practical consequences*. Al-Cu-Fe and Al-Mn-Pd offer some complementary possibilities, which we have used to reach a global coverage of all aspects of atomic hopping in QCs: isotopic substitution has been performed in the system Al-Cu-Fe, where we were restricted to the use of powder samples. On the other hand, no isotopic contrast is at hand in Al-Mn-Pd, but we have been able to make an extensive triple-axis neutron scattering study on large single grains, which we are reporting here. It may be worth noting that in decagonal systems, it has become possible recently to combine both approaches in one system: In Al-Co-Ni large single-grain samples can now be produced by floating-zone[57] or flux-growth[58] methods and there are opportunities for isotopic substitutions in the Ni element.

III. SYNOPSIS OF PREVIOUS RESULTS OF HOPPING STUDIES

In this section we would like to present a short chrestomathy of previous results. The aim is to provide the reader with some necessary background. The intensities and the widths of the Lorentzian signals that occur in the quasielastic structure factors such as given by Eq. (1) can be studied as a function of **Q**, temperature T, and isotopes. The **Q** dependence contains information about the geometry of the jumps, the T dependence about the energetics of the jumps, and the isotopic dependence about the atomic species involved in the jumps.

The isotopic studies in Al-Cu-Fe by neutron scattering[1,5] and by Mössbauer spectroscopy[2,4] revealed that Al, Cu, and Fe are jumping on different time scales. At least four different characteristic times have been detected. Each of these jumps was further documented in terms of its T and **Q** dependence. (Some results on approximant phases with natural isotopic compostions were obtained as well.) All this is summarized in Table II. The prime interest of the isotopic results is that they vindicate our interpretation of the quasielastic signals in terms of phason hopping. As this assignment was anathema for a long time,[65] it is worth reminding the reader of its justification. Quasielastic Lorentzian-shaped signals as observed by neutron scattering can in principle arise from (1) experimental artifacts such as the presence of hydrogen in the sample, (2) paramagnetism, (3) an (exotic) vibrational density of states, (4) rotational diffusion of molecules, (5) melting of the sample, (6) translational diffusion, or (7) local atomic jumps. A number of these possibilities can be discarded based on specific arguments. E.g., paramagnetism is not probable in our samples since they have been checked by superconducting quantum interference device (SQUID) measurements, which revealed that they were not magnetic. Moreover, the quasielastic intensity does not follow the required typical magnetic form factor. Finally the temperature dependence of the quasielastic signals can not be explained easily in terms of magnetic interactions within the sample. But the isotopic results address almost all the issues (1)–(7)

simultaneously. The 55-μeV-wide quasielastic signal that has been measured in isotopically enriched and natural samples of Al-Cu-Fe had an intensity that was directly proportional to the *nuclear* Cu *cross section* in the sample. It can thus not be due to hydrogen (which has a different cross section), paramagnetism (which should follow a *magnetic* cross section), a density of states, or melting of the sample (which should involve all atomic species on comparable time scales). Rotational diffusion of molecules can be excluded on physical grounds (viz., binding energies), such that an interpretation of the results in terms of atomic hopping is the only possibility left over. It remains at this stage then an open question whether this hopping entails long-range translational diffusion or otherwise. In view of these arguments the existence of phason hopping has now been universally accepted within the QC community[65–69] (see also Appendix A).

As mentioned above, the results in Table II can be used (with due precaution) to develop some sense of the nature of the atomic jumps in Al-Mn-Pd, where similar jump times have been identified.

Both in Al-Cu-Fe and in Al-Mn-Pd powder experiments the T dependence of the quasielastic signals systematically reveals the same unusual behavior. It is equally manifest in the decagonal phase Al-Co-Ni (Ref. 8) and even in the localized hydrogen dynamics within the compounds TiNiZr-H.[70,71] It has been interpreted in terms of *assisted* hopping. The intensity $\mathcal{I}$ of the Lorentzian quasielastic hopping signal exhibits an Arrhenius law, while its width Γ is practically constant with temperature. This is the opposite of the conventionally observed temperature dependence, where it is Γ that shows an Arrhenius behavior and $\mathcal{I}$ that remains constant with T. This statement applies to both localized hopping and long-range translational self-diffusion. In Ref. 72 a model for the assistance has been developed and discussed. In this assistance scenario, the atom that is a candidate for jumping is arrested in front of a ''closed door'' (which is typically a high-energy barrier). The energy necessary to open the door is called the assistance energy. Once the door is open the atom can jump lissomely between the two sites of the double well, since now it has to leapfrog only a very low residual potential-energy barrier. At low temperatures, most of the local atomic configurations are locked. When the temperature increases, the assistance mechanism is activated, and the *number* of favorable configurations (excited states where the jump has become possible) increases, giving rise to an increase of quasielastic intensity. The assistance energies extracted from the Arrhenius-like plot for the intensities span the range of values from 150 meV to 750 meV, such that they are compatible with assistance mechanisms based on phonons or phason clouds.

IV. PREPARATION OF THE EXPERIMENTS

It is not realistic to begin a triple-axis neutron-scattering experiment without some preliminary studies. We have therefore based our search strategy on two golden rules of conduct: (a) performing first a global prospecting search in reciprocal space by TOF quasielastic-neutron-scattering experiments on powders and (b) nailing down as much as possible the signals expected by various model calculations. We will now dwell on both aspects of this preparation.

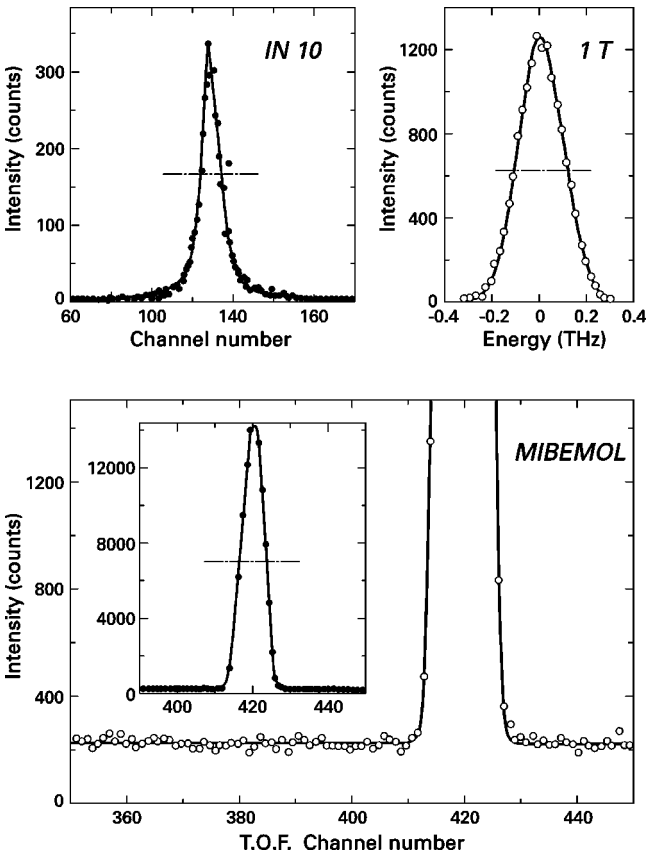

FIG. 1. Comparison of the elastic resolution functions of a number of instruments designed for inelastic neutron scattering: the time-of-flight spectrometer MIBEMOL (LLB, Saclay), the backscattering spectrometer IN10 (ILL, Grenoble), and the triple-axis spectrometer 1T (LLB, Saclay). Note that the two latter (which use crystals for energy selection) exhibit wings, while a zoom onto the foot of the resolution function of MIBEMOL shows an almost vertical edge, which offers a very precise distinction between elastic and inelastic scattering.

A. Exploratory TOF survey

(a1) In a triple-axis or backscattering spectrometer the resolution function has a physical origin, viz., the Bragg reflection from a crystal. Consequently, it is not triangular and one can hit a problem of ''contamination of the signal by elastic scattering'' for small energy transfers, due to the mosaicity of the crystal. This contamination can become a major obstacle if one wants to discern weak signals in the vicinity of strong Bragg peaks. In sharp contrast hereto, the shape of the resolution function of a TOF spectrometer such as MIBEMOL is triangular as its origin is predominantly geometrical or mechanical. It stems from the passing of the chopper window through the neutron beam. Signal-to-noise ratios S/N of 10 000:1 can be achieved, which means that a signal as weak as 10^{-4} times the elastic peak can be detected just next to its foot. Such ghostly signals will almost certainly elude detection on a triple-axis spectrometer or on a TOF spectrometer using crystals for energy selection. These arguments are illustrated in Fig. 1, which shows the resolu-

tion functions for a representative choice of spectrometers. In the worst possible case one might even be constrained to work with an oriented single-grain sample on a TOF spectrometer, sacrificing on the **Q** resolution.

(a2) A triple-axis spectrometer is also very selective in **Q** space. Before zooming into a particular location in reciprocal space it is instrumental to take first a global ''picture'' on a TOF spectrometer in order to get a crude idea on where to start looking (somewhat in the same way as a powder diffraction experiment prepares a run on a four-circle diffractometer). This can be already time consuming in its own right: whereas runs with an incident neutron wavelength of 8 Å were quite successful in our study of Al-Cu-Fe, they were not with Al-Mn-Pd,[6] and it took patiently varying the relevant parameters in order to figure out the proper experimental conditions for the investigation of the quasielastic signals. Even if one were looking at the right place, on a triple-axis spectrometer the signal could still be overlooked if the energy width of the constant-**Q** scan were chosen too narrow with respect to the width of the quasielastic signal.

To summarize these two points related to our first rule of thumb: In the initial stages, the serendipity to spot quasielastic signals will be greatly enhanced by making first exploratory surveys on powder samples with a TOF spectrometer. Without such prior information the whole exercise might start looking like a search for the proverbial needle in a haystack. We have made these prerequisite experiments, and reported them in Ref. 6. The ensuing results have taught us the following: (1) The quasielastic intensity is more intense at large **Q**. In particular, no signal could be detected below $Q=2$ Å^{-1}. (2) The energy scans must cover at least the interval $[-0.7,0.7]$ meV. Indeed two signals have been observed: a wider one with $\Gamma_1=700$ μeV and a narrower one with $\Gamma_2=200$ μeV. (3) The energy resolution has to be good enough to render the observation of a 200-μeV-wide signal feasible. On the other hand, one will be forced to degrade this resolution when one wants to measure the wider component. To satisfy both criteria the triple-axis spectrometer has been used in two different configurations (see below). The best conditions are achieved with final wave vectors $k_f=1.64$ Å^{-1} ($\Delta E=100$ μeV) and $k_f=1.97$ Å^{-1} ($\Delta E=200$ μeV). Keeping the final wave vector constant has the advantage that one works with constant detector efficiency.

B. Heuristic jump models

Our second golden rule is motivated by the following considerations.

(b1) We must insist on the fact that the **Q** window for the observation of phason dynamics be dictated by a quasielastic structure factor such as expressed, e.g., in Eq. (1). The premise for this statement is the hopping paradigm for phason dynamics advocated in the Introduction, which has been firmly established by the previous results of our work, related in Sec. III. Searches for phason hopping by de Boissieu and co-workers[73] on the triple-axis spectrometer 4F2 of the L.L.B. in Saclay and on the backscattering spectrometer IN16 of the I.L.L. at about 1.55 Å^{-1} took guidance from the presence in that region of diffuse scattering attributed to phason strain that disappeared gradually (but reversibly) at high temperature. This kind of search strategy would be invaluable in a soft-mode scenario for a structural phase transition, but it constitutes a counterproductive sidetrack in the case of phason dynamics in QCs (Ref. 74) since it starts from the wrong image. One cannot seriously uphold the idea of a quest for additional or alternative scripts of the phason dynamics, as we have amply pleaded in Ref. 72: In reality, the diffuse scattering will appear in all together different places in **Q** space than the signature of the phason dynamics. Also technically, such an approach bears little chance of success. As has already been pointed out above, the presence of strong elastic scattering is more a nuisance than anything else during a search of quasielastic signals on a triple-axis spectrometer.

(b2) Figure 2 shows the results (under the form of contour plots) of calculations of the quasielastic structure factors for the most simple models of atomic jumps along twofold, threefold, and fivefold directions, taking the corresponding lengths of the jump vectors from the model of Katz and Gratias.[19] They just materialize the philosophy that if a jump occurs along an axis of symmetry, an equivalent jump must also occur along every other axis of the same symmetry. Thus we have calculated sums:

$$S_{qel}(\mathbf{Q})=\frac{1}{2}\sum_{i=1}^{n_s}[1-\cos(\mathbf{Q}\cdot\mathbf{d}_i)], \tag{2}$$

where $\mathbf{d}_i$ are the $n_s=30/s$ jump vectors along the s-fold directions. Each term $\frac{1}{2}[1-\cos(\mathbf{Q}\cdot\mathbf{d}_i)]$ is a structure factor for a single jump between two (energetically) equivalent sites separated by a jump vector $\mathbf{d}_i$. Also shown in Fig. 2 are the symmetry axes of the QCs and three concentric circles corresponding to $Q=\pi/d$, $Q=3\pi/2d$, and $Q=2\pi/d$. The middle one ($Q=3\pi/2d$) corresponds to the relation between jump distance and Q in a powder sample. These models assume that the neutron-scattering process is incoherent, which in general may be a fallacy: e.g., in the case of Al-Cu-Fe, the Cu signal observed in the 50–200 μeV resolution range is mainly coherent. Therefore, we also engaged in calculations of a model for coherent scattering signals, with jumps along twofold directions, taking into account the correlations between various atoms.[75] It is inspired by the model of Katz and Gratias,[19,38] which foresees that the Cu atoms in Al-Cu-Fe build constellations of 7 atoms distributed over the 20 vertices of a dodecahedron according to two simple rules: (1) two Cu atoms should never be first neighbors, and (2) two Cu atoms should never occupy opposite positions on the dodecahedron. All jumps are allowed provided these two rules remain always respected. The jumps in this model occur along the edges of the dodecahedron, i.e., along twofold directions. The various possibilities for the atomic jumps take the system on a trip through a configuration space that contains in all 100 members only. The detailed elaboration has been decribed elsewhere.[75] Its results for one specific (but immaterial) choice of jump times are shown there in a figure. Comparison with Fig. 2(a) shows that the refinement obtained by adding longer-distance correlations into the model entails only minor corrections.

Moreover, if the assistance scenario is the correct explanation for the anomalous temperature dependence of the quasielastic signals, then this may provide us with a second

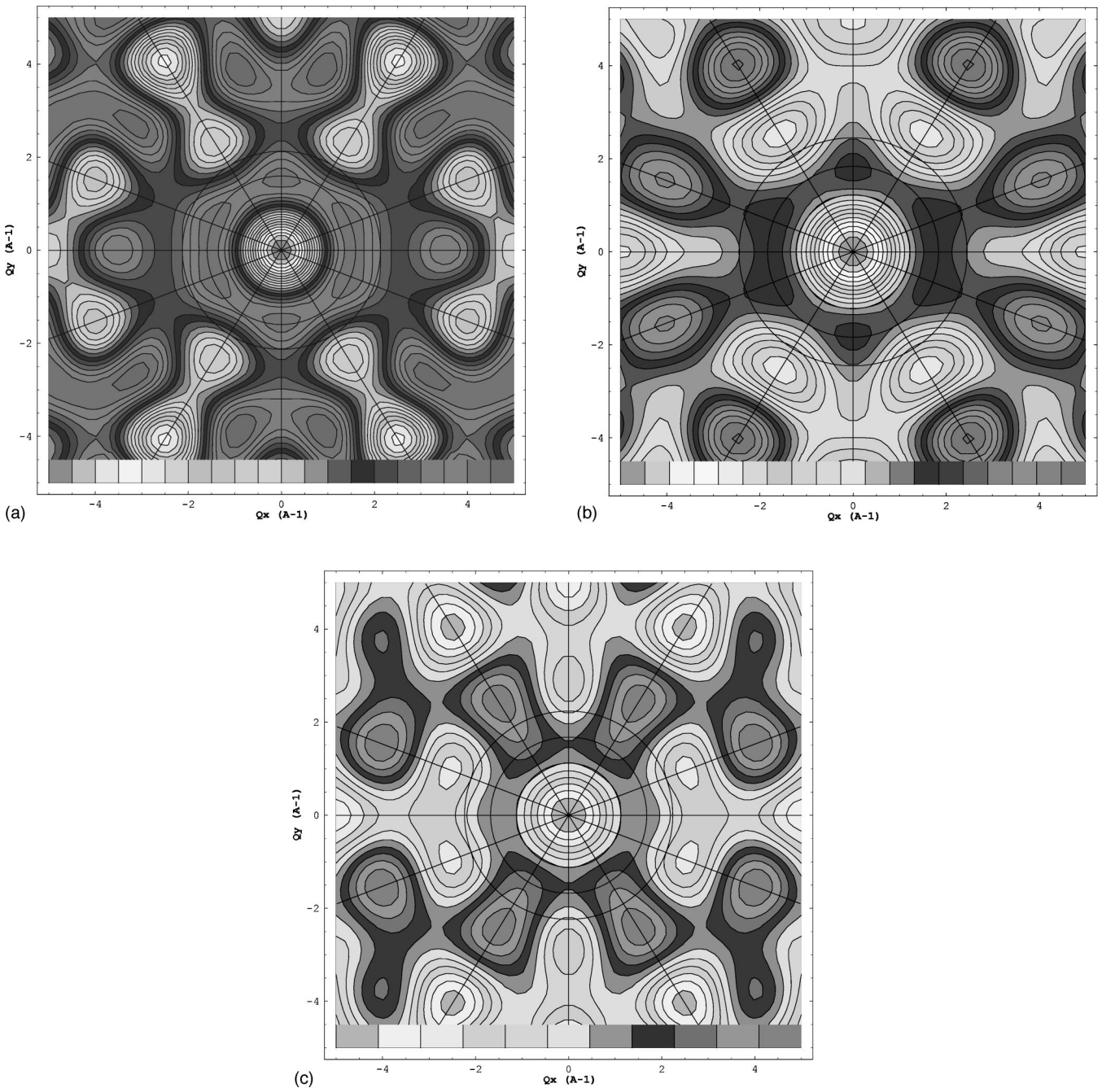

FIG. 2. Contour plots of quasielastic structure factors for simple models of jumps in symmetric double-well potentials oriented along (a) twofold (jump distance $d=2.95$ Å), (b) threefold ($d=2.56$ Å), and (c) fivefold ($d=2.8$ Å) axes, as described in the text. The three concentric circles correspond to $Q=2\pi/d$, $Q=3\pi/2d$, and $Q=\pi/d$. The twofold, threefold, and fivefold axes are also shown. The contour lines correspond to integer numerical values, with increments of 1. The greyscale code is shown at the bottom of each figure, going from left to right; e.g., the first shade on the left codes numerical values between 0 and 1.

motivation to stick to the more simple models. Indeed, it may take a long time to build up the favorable environment that unlocks a given jump between two neighboring sites. The opportunities for the assisted atom to leap even further to a second-neighbor position could be very few and far between, as in principle they require two assistance conditions to be fulfilled simultaneously. Consequently, within the model of 100 constellations alluded to above, the time behavior will no longer be represented by the exponential of the 100×100 jump matrix we calculated numerically in Ref. 75 since the underlying treatment foregoes the possibility of an assistance mechanism. The intermediate quasielastic scattering function $S(\mathbf{Q},t)$ will to a good approximation be an incoherent sum of one-Lorentzian structure factors $\langle\mathcal{F}_j(\mathbf{Q},t)\mathcal{F}_k^*(\mathbf{Q},0)\rangle$, where $\mathcal{F}_j(\mathbf{Q},t)$ is the Fourier transform of a configuration with label j at time t, and the two configurations j and k can be obtained one from another by a single atomic jump. The effect of assistance to the jump process should tend to make the second-order correlation times, corresponding to processes that comprise more than one step on

the connectivity diagram in configuration space, inaccessibly long. Solely the simplified models have thus been used as a guide for the searches of quasielastic intensity.

As can be appreciated from Fig. 2, for *all* types of jumps there is an intensity maximum in the form of a spherical shell at about 1.7 Å^{-1}. If these calculations mirror more or less adequately the experimental situation, then quasielastic data taken on a single grain at these **Q** values will not be of any more use than a TOF run on a powder sample, since the data are isotropic and do not allow one to make a discrimination between the various types of jumps. Very strong anisotropy will only show up around 3 Å^{-1}.

V. EXPERIMENTAL PROCEDURES

The single-grain samples have been prepared at C.E.C.M. Vitry by the Czochralsky method. Their structural quality has been controlled by neutron diffraction (Laue method), and they were checked to be monophasic. Two single-grain samples have been used. Unfortunately, the larger one became only available in a relatively advanced stage of the experiments. The smaller one has dimensions $35\times11\times7$ mm^3. It is the same sample as described in the diffuse scattering studies by Caudron *et al.*[76] The larger one was more or less conical in shape with a base of 15 mm diameter and a height of 50 mm. The composition of the samples was $Al_{70.4}Pd_{21.0}Mn_{8.6}$. Measurements with a SQUID magnetometer on specimens of identical composition have shown that the phase studied is not magnetic.[77] This is further borne out by the absence of a quasielastic (paramagnetic) signal at room temperature. The samples were cemented onto boron-nitride supports and installed under vacuum (better than 10^{-6} mbar) inside a furnace enabling a temperature regulation to an accuracy of 1–2 °C.

The experiments have been performed on the graphite-double-monochromator triple-axis spectrometer 4F2 installed at a cold-neutron beam port of the Orphée reactor of the L.L.B. at Saclay, France. The spectrometer was used in the fixed final-wave-vector (k_f) configuration. A graphite filter was used on the scattered beam to suppress contamination from higher harmonics. The data were taken using a curved (PG 002) analyzer, in order to increase the counting rates. This results in some loss in Q resolution, which is entirely acceptable for our kind of study, where a rather slow variation with **Q** of the signal can be anticipated.[78] The setup is equivalent to horizontal collimations of 25/25/48/48 min in the Cooper-Nathans formalism.[79] The energy step in the scans (0.025 THz) was adapted to the energy resolution.

The samples were aligned in the beam in such a way that the horizontal scattering plane of the instrument correponded to the superior right quarter of a binary plane of the QCs (as can be seen in Fig. 3). Such a quadrant contains all types of high-symmetry axes of the system, and is perpendicular to a twofold axis. The two twofold axes within the scattering plane define the coordinate axes (Q_x, Q_y) in reciprocal space. The more intense Bragg peaks of the Al-Mn-Pd system are also indicated in the figure. As already mentioned, one has to avoid as much as possible to venture into the close neighborhood of these peaks because they are prone to induce an important elastic contamination of our data. Moreover, the presence of strong coherent signals from the acoustic phonons (whose intensities scale with the intensities of the Bragg peaks) would also hamper a clean data acquisition. [We may note that the quasielastic intensity is very small (1–5 %) compared to the diffuse elastic scattering far from the Bragg peaks, which itself is of the order of 1% or less of the Bragg intensities.]

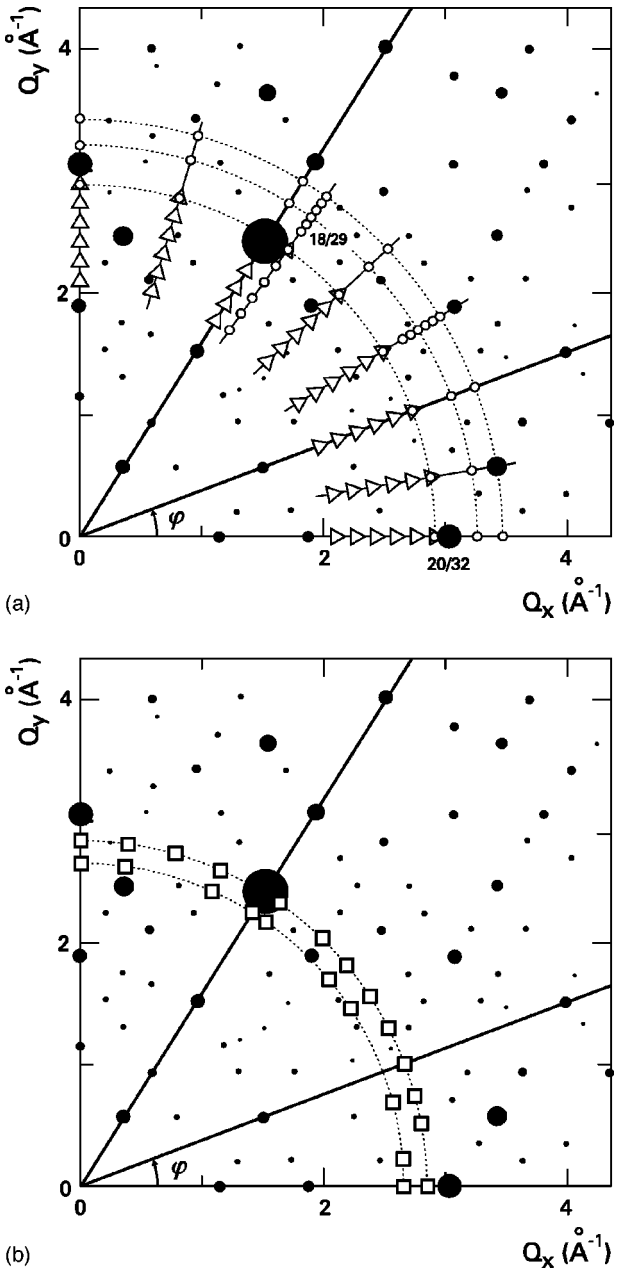

FIG. 3. Binary scattering plane. Bragg peaks are flagged by solid circles, whose diameter is proportional to the intensities. Open circles ($k_f=1.97$ Å^{-1}, small sample), triangles ($k_f=1.64$ Å^{-1}, small sample), and squares ($k_f=1.64$ Å^{-1}, large sample) are measured points. This plane is the same as in Fig. 2.

We carried out four series of experiments, amounting to a total beam time of 2 months. The use of two different configurations affords the inspection of a large slice of reciprocal space, ranging from 2 to 3.4 Å^{-1}. The experimental points corresponding to the constant-Q scans on the small sample in the configuration $k_f=1.64$ Å^{-1} are plotted as triangles, while open circles tag the measurements made in the

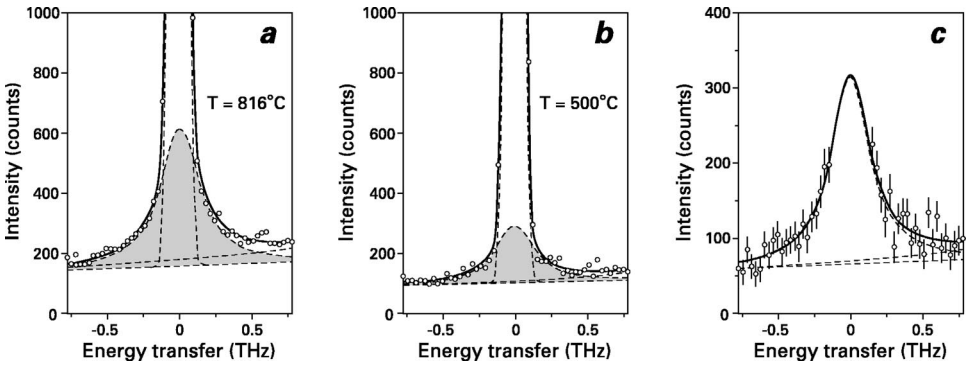

FIG. 4. Validation of the presence of quasielastic scattering: (a) High-temperature data. The shaded area corresponds to the quasielastic component. (b) Low-temperature data. The quasielastic signal has almost disappeared. (c) Subtracted data, clearly evidencing the existence of a quasielastic contribution.

configuration $k_f = 1.97$ Å^{-1}. Open squares situate the scans made on the large sample in a $k_f = 1.64$ Å^{-1} setup. At each point we collected an energy spectrum measured between -0.7 and 0.7 meV, at two temperatures: 500 °C [low temperature (LT)] and 800 °C [high temperature (HT)]. (In the experiments on the larger sample the LT runs were carried out at 400 °C rather than at 500 °C, as we had learned from the expierence gained with the small sample that some residual quasielastic signal still survives at 500 °C.) The purpose of the low-temperature runs was to validate the presence of quasielastic intensity at high temperature by a subtraction method. In fact, as outlined in Sec. IV, it can in principle be hard to tell apart a quasielastic signal from the wings of the elastic resolution function. In a subtraction of the low-temperature data from the high-temperature data, such wings should show up as negative intensity (due to the Debye-Waller factor), while the presence of quasielastic intensity should be revealed by a positive signal (see Fig. 4). The low-temperature run thus serves as a background measurement. After each change of temperature the 20/32 Bragg peak was scanned in θ-2θ mode in order to monitor the dilatation effects in the lattice parameters. These were then automatically corrected for in the subsequent scans. Typical run times of a scan were of the order of 4 h for 51 data points. Some more demanding scans, in points with very weak quasielastic intensity, lasted for 8 h. The size of the incoming beam was reduced by vertical and horizontal diaphragms such as to optimize the signal/noise ratio between the scattering from the sample and from its environment.

The fit procedures are very sensitive to the background levels (see below). Therefore we measured directly the incoherent background by selecting a point at $\omega = -0.13$ Thz in energy and counting the total intensity as a function of temperature. Several points $(\mathbf{Q},\omega)$ were included in this evaluation of the $\mathbf{Q}$ dependence of the background. Figure 5 illustrates the method. Two distinct temperature regimes can be clearly observed: at low temperatures the intensity follows a linear law. The phason jumps are not yet activated, and only the incoherent phonon background contributes to the signal. At high temperatures, the intensity is the sum of the background signals and the quasielastic intensity arising from the jumps. By extrapolating the low-temperature law in a harmonic approximation, one can quantify the incoherent contribution at high temperature. The raw data can then be fitted more reliably by using this information. The difference between the high- and low-temperature readings of the incoherent background gives the values that must apply for them in the fits of the HT-LT subtracted data sets (see below). Figure 6 shows the $\mathbf{Q}$ dependence of the background levels as a function of Q^2. The law runs linearly at small Q, and then bends off as it is modulated by the Debye-Waller factor. We might mention in passing that the incoherent phonon background in a single-grain sample need not always to be isotropic. This is due to the way the neutron scattering intensity is related to the atomic motion by a coupling term $\mathbf{Q}\cdot\mathbf{e}_p$ [which also occurs in Eq. (1)], where $\mathbf{e}_p$ is the polarization vector of the phonon.

VI. DATA ANALYSIS

A. Basic philosophy

The data analysis is performed in several consecutive steps.

(1) The first parameter to determine is the quasielastic width $\Gamma(\mathbf{Q})$. Preliminary fit results indicated that the signals could be analyzed keeping $\Gamma(\mathbf{Q})$ constant and equal to its mean value for a given value of Q. In a first approach the representation of the data by a single Lorentzian component has to be seen as a convenient *ad hoc* parametrization. It cannot be excluded *a priori* that more than one width could

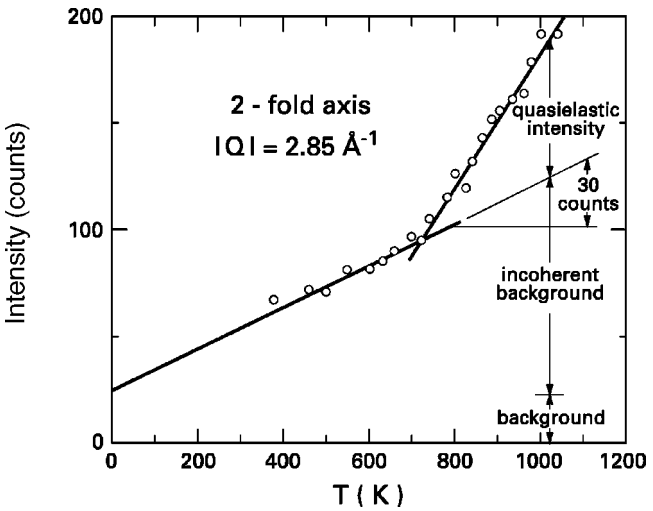

FIG. 5. Determination of the incoherent phonon background. The intensity at point ($|\mathbf{Q}| = 2.85$ Å^{-1}, $\omega = -0.13$ Thz) on the twofold axis as a function of temperature. At high temperature the signal consists of a constant background, an incoherent background, and the quasielastic signal. The difference between the intensities at 800 and 500 °C is 30 counts.

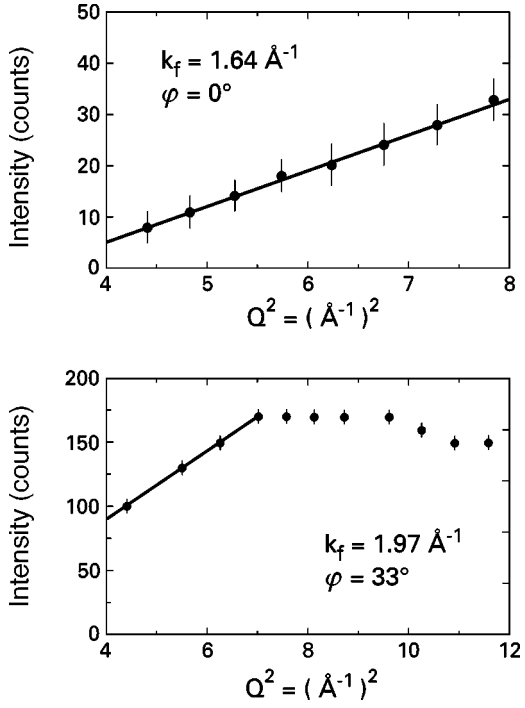

FIG. 6. Background vs Q^2. In the measurements in the $k_f = 1.64$ Å^{-1} setup the dependence is linear. At larger Q values the Debye-Waller factor enters the game.

be present at a given value of **Q**, but the statistics and the resolution hamper the extraction of such detailed information from the data.

(2) By comparing the intensities of the points located on a same crown of constant $|\mathbf{Q}|$, it is possible to study jump anisotropies. We focused our attention on the intensities on four crowns: $|\mathbf{Q}| = 2.65$ Å^{-1}, $|\mathbf{Q}| = 2.85$ Å^{-1}, $|\mathbf{Q}| = 3.2$ Å^{-1}, and $|\mathbf{Q}| = 3.4$ Å^{-1}. The crown at 2.85 Å^{-1} has been studied in the two k_f configurations and with two samples. The motivation herefore was to check the experimental methods and to evaluate the influence of resolution effects on data treatment.

(3) By grouping points belonging to the same symmetry axis (or the same radial line between symmetry axes), it is possible to determine radial intensity profiles, which are important for the evaluation of the jump distances. Measurements at $k_f = 1.64$ Å^{-1} covered the region between 2 and 2.85 Å^{-1}. Measurements at $k_f = 1.97$ Å^{-1} extended this area upwards to 3.4 Å^{-1}. As mentioned before, overlapping zones should (at least in principle) allow one to cross-check the data on reliability and reproducibility.

(4) After grouping together and analyzing the data, an interpretation in terms of atomic jumps can be envisaged by comparing the results to the model calculations of Sec. IV. Each intensity profile—radial or along a crown—is compared to the theoretical profile obtained from jump simulations along twofold, threefold, and fivefold axes [Eq. (2)].

These are the ingredients for the data analysis. However, complications in the fit procedures arise due to two circumstances: (1) The presence of other components than the quasielastic signal in the spectra, viz., the (very strong signal of the) elastic peak and a (also rather strong) phonon background, and (2) the possibility that there could be more than one quasielastic signal.

B. Elastic and phonon background

The correlation between the fit parameters of the strong elastic and the weak quasielastic signals introduces huge uncertainties in the determination of the quasielastic widths and intensities. To avoid an optimization of the elastic peak parameters at the detriment of those of the quasielastic line, it is necessary to exclude the elastic peak from the fits. The width Γ of the quasielastic signal can then in principle be determined with good precision. Nevertheless, the fits on the raw data can remain tricky (e.g., due the presence of the phonon background). We have tried also to fit the subtracted data sets: In the subtraction of a low-temperature run from a high-temperature run, the quasielastic component is not affected, but incoherent or coherent phonon backgrounds can to a great extend be eliminated. In the central-peak region, the result of the subtraction is negative due to the Debye-Waller factor. The fit is thus done only on the wings of the Lorentzian signal, as shown in Fig. 4. But the drawback of a fit to a subtracted data set is that the statistical accuracy is severely impoverished. The anisotropy of the intensity can no longer be detected within the statistical precision as shown in Fig. 7 at $Q = 2.85$ Å^{-1}, which may be compared to the nonsubtracted data shown in Fig. 8.

C. One or two Lorentzians

In a first step we analyzed all raw spectra with a single Lorentzian component. The $k_f = 1.64$ Å^{-1} data indicated the presence of a 400-μeV-wide signal. Figure 9 shows the **Q** dependence of Γ on a crown and along the Q_x axis. Taking into account that values obtained at low **Q** tend to be slightly underestimated due to the weakness of the signal, it appears that the width does not vary with Q. This value of 400 μeV confronted us with a thorny problem. In our earlier work on powder samples with the TOF spectrometer MIBEMOL (Ref. 6) we reported two signals with widths $\Gamma = 200$ μeV and $\Gamma = 700$ μeV, respectively. The intermediate value of 400 μeV obtained from the $k_f = 1.64$ Å^{-1} triple-axis data thus suggested that it could result from the presence of both contributions within the spectrum. The triangular resolution function of the TOF spectrometer is certainly better suited for a precise determination of a width. However, with a single-grain sample the coherent phonon background is confined to a single specific place at each **Q** value, and one can spot many **Q** values where it does not spoil the corresponding energy scan at all. In the TOF data the phonon problem becomes really bothersome at higher Q values. After scrutiny of all elements we finally reached the following conclusions: (1) The 200-μeV-wide component observed with MIBEMOL is so weak that it escapes detection in the triple-axis scans under the present conditions of resolution. (2) The width of the wide component cannot be determined reliably from the TOF data, due to a lack of statistics and due to a genuine problem of phonon background contamination. The MIBEMOL data are equally well fitted with any value for the width in the range 400–700 μeV. (3) Given the excellent quality of the fits in the $k_f = 1.64$ Å^{-1} triple-axis data at 2.85 Å^{-1} we conclude that the best value for Γ is 400 μeV. We must thus admit that our quotation for this width in Ref. 6 has not been sufficiently cautious and is in error. These conclusions are further corroborated by the k_f

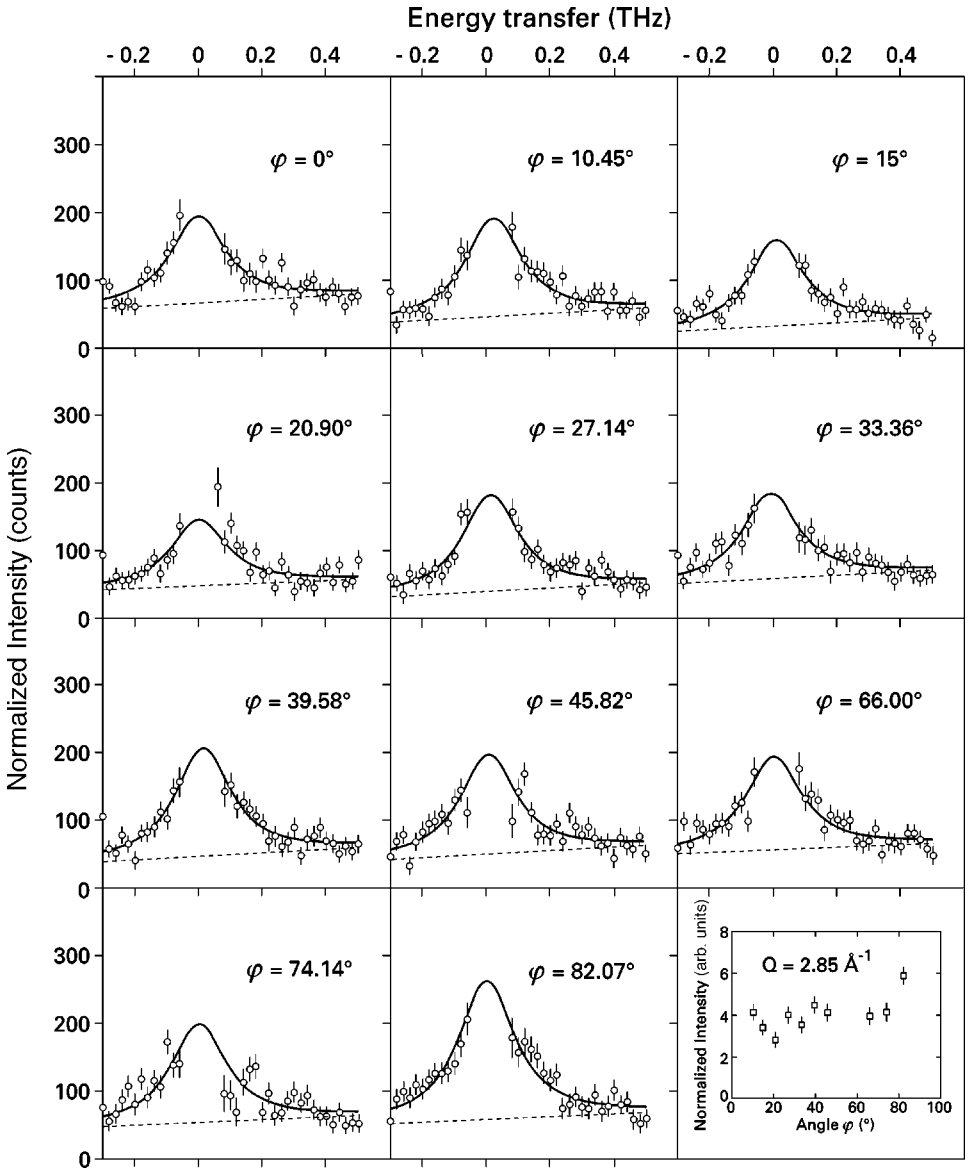

FIG. 7. Analysis of the subtracted data on the crown at $|\mathbf{Q}| = 2.85$ Å^{-1} in the the $k_f = 1.64$ Å^{-1} experimental setup. The data were obtained on the large sample. The anisotropy can no longer be detected within the statistical precision. This is also true of subtracted data obtained on the small sample with $k_f = 1.97$ Å^{-1}.

$=1.97$ Å^{-1} data. First of all, they could also be fitted with this value, and furthermore at $Q=2.85$ Å^{-1} they resulted in the same angular dependence of the intensity, as can be verified in Fig. 10. Moreover, the possibility that the $k_f = 1.97$ Å^{-1} data could contain some contribution from the 200 μeV component can be dismissed on the basis of the resolution which is too coarse.

D. Trials of a two-Lorentzian analysis

We may mention that in order to tackle the dilemma of the number of Lorentzians we also tried to fit our data with two Lorentzian signals ($\mathcal{L}_1$ and $\mathcal{L}_2$). Unfortunately, the weak intensities preclude such an analysis, leaving the parameters completely free, and the fit program does not converge. Therefore, we were forced to perform the two-Lorentzian fits keeping the width parameters fixed. We choose $\Gamma_1 = 200$ μeV and $\Gamma_2 = 700$ μeV on the basis of Ref. 6.

The $k_f = 1.64$ Å^{-1} data. Figure 11 shows that the best fit is obtained with a combination of $\mathcal{L}_1$ and $\mathcal{L}_2$, with a dominating contribution arising from the narrow component. Analyzing the same data with $\mathcal{L}_1$ alone, or $\mathcal{L}_2$ alone, leads to less satisfactory results.

The $k_f = 1.97$ Å^{-1} data. A fit with two components is good, but *a comparable agreement with the data can be obtained considering only the wide component*. On the other hand, the 200 μeV signal alone is not suitable. This is illustrated in Fig. 12.

However, in such a two-component analysis, the results for the intensity of the wide component in the two k_f setups at $Q=2.85$ Å^{-1} no longer match. This is a further validation of our one-Lorentzian analysis.

VII. RESULTS

A. Crowns of constant Q

1. $Q=2.85$ Å^{-1}: Comparison of the three experimental setups

The crown at $|\mathbf{Q}| = 2.85$ Å^{-1} has been measured three times, under different conditions, to check the reproducibility of the data. It was measured at $k_f = 1.64$ Å^{-1} and $k_f = 1.97$ Å^{-1} with the small sample and at $k_f = 1.64$ Å^{-1} with the large sample. The $k_f = 1.64$ Å^{-1} data for the large sample with the corresponding fits are shown in Fig. 8. The $k_f = 1.97$ Å^{-1} data with their fits are shown in Fig. 10. The

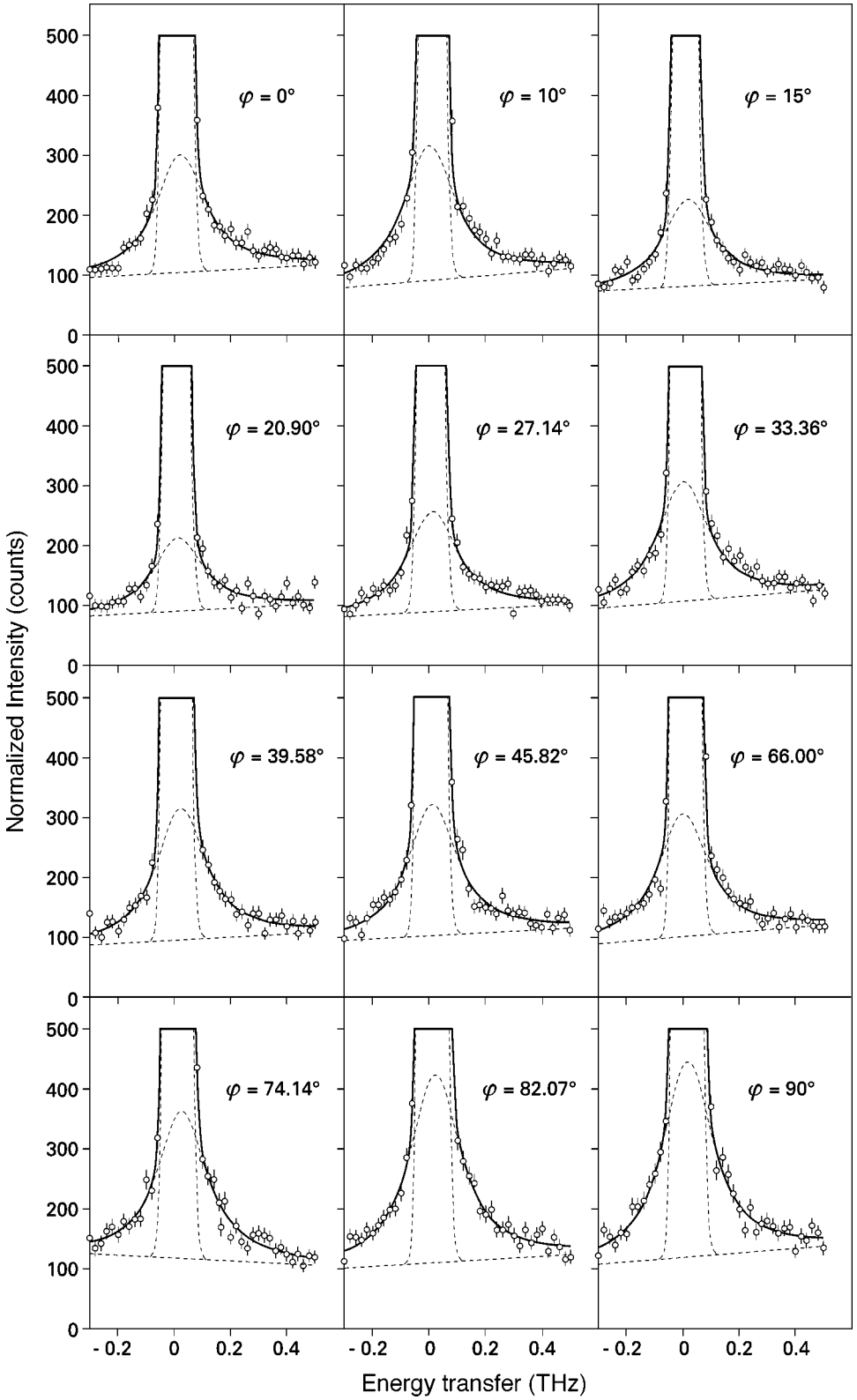

FIG. 8. Panorama of the non-subtracted data on the crown at $|\mathbf{Q}|=2.85$ Å^{-1} in the the $k_f=1.64$ Å^{-1} experimental setup. These data were obtained on the large sample and the analysis shown leads to the intensity plot of Fig. 13.

same general shape is observed in the two different k_f setups. It is typified by strong minima on the fivefold and threefold axes, as shown in Fig. 13.

2. Results on other crowns

In the same Fig. 13 we show similar results for the crown at $Q=2.65$ Å^{-1} ($k_f=1.64$ Å^{-1}) obtained with the large sample. Again minima are observed on the fivefold and threefold axes.

The other crowns ($Q=3.20$ Å^{-1} and $Q=3.40$ Å^{-1}) were measured in the $k_f=1.97$ Å^{-1} setup with the small sample. The spectra are shown in Figs. 14 and 15. The fits at $Q=3.20$ Å^{-1} were difficult and the values for the intensities are more qualitative in nature than at 2.65 and 2.85 Å^{-1}. Disentangling the phonon background faces insuperable odds at 3.4 Å^{-1} such that for this value only the raw data are shown. An important point to be stressed is that already in the 3.2 Å^{-1} data the tendencies in the φ dependence are

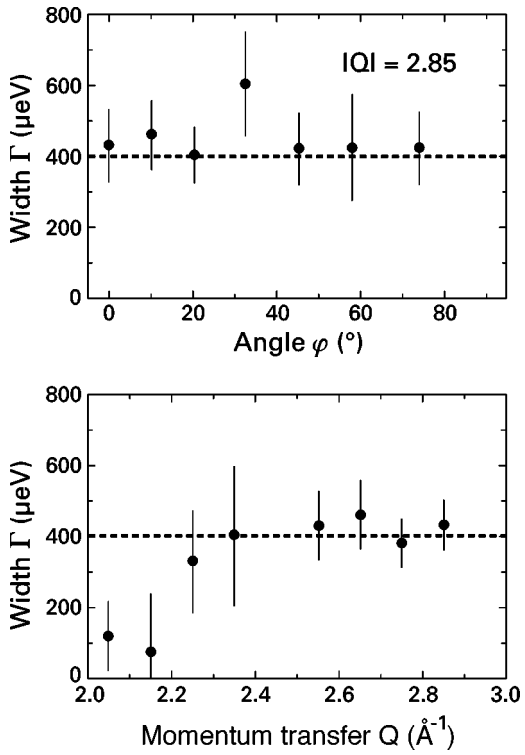

FIG. 9. **Q** dependence of the Lorentzian width Γ. Left: on the $|\mathbf{Q}|=2.85$ Å^{-1} crown. Right: along a twofold axis. The width is constant within the experimental precision and equal to 400 μeV. Data taken with small sample.

completely inverted with respect to those observed at 2.85 Å^{-1}. The angular dependence now shows maxima on the fivefold and threefold axes.

In conclusion, two angular profiles with distinct shapes have been observed.

B. Radial profiles

The radial profiles seem to be much less sensitive to details of the fit procedures. They could still be deduced from subtracted data sets. We present results obtained with the small sample.

$k_f=1.64$ Å^{-1} *data*. Figure 16 gives the results obtained along various radial axes. The intensity grows continuously with the modulus of **Q**, but the *Q* window is not wide enough to reach a first local maximum. Only the measurements on the twofold axis indicate the existence of such a maximum around $|\mathbf{Q}|=2.7$ Å^{-1}.

$k_f=1.97$ Å^{-1} *data*. The main interest of this second configuration is to extend the *Q* range up to 3.4 Å^{-1}. Figure 17 evidences how a local maximum is reached on the twofold, threefold, and fivefold axes, and also along some intermediary direction between the threefold and fivefold axes, for which the maximum is particularly well marked at $|\mathbf{Q}|=2.8$ Å^{-1}. Figure 18 shows the corresponding spectra. Although this ensemble of data was polluted by a phonon contribution on the right hand side, the fit remained possible. In other cases, for instance, on the threefold axis, only a few points could be analyzed. Moreover, no study along the fivefold axis could be performed due to the presence of the 18/29 Bragg peak (a radial dependence has been measured close to this axis, viz., at $\varphi=55°$).

Data comparison. Figure 19 compares the radial profile on the twofold axis obtained with both experimental setups. After intensity normalization, the results appear to be concurrent, both evidencing the existence of a local maximum around 2.7 Å^{-1}. This agreement further comforts us in our strategy to confine ourselves to a treatment based on a single Lorentzian contribution.

VIII. DISCUSSION

A. Single-particle models

We now would like to verify if the single-particle models delineated in Sec. IV [Eq. (2)] are able to provide a consistent description of our data. The first approach consists in comparing the data to the models in a simplified fashion: with models corresponding to a unique variety of jump, either along twofold, threefold, or fivefold directions. If this does not lead to satisfactory results (and we will shortly see that this is the case), we must allow for the fact that a number of different jumps may coexist in a spectrum, such that each intensity profile results from the combination of several elementary jumps. The number of jumps to be taken into account, their distances, their directions, and their relative abundances are all unknown. The theoretical intensity must then be expressed as

$$\mathcal{I}_{qel}(\mathbf{Q})=\sum_i \alpha_i \mathcal{I}_i(d_i,\mathbf{Q}), \tag{3}$$

where α_i denotes the abundance and $\mathcal{I}_i(d_i,\mathbf{Q})$ the quasielastic intensity for a class of jumps *i* with symmetry s_i over a distance d_i. We must of course obtain a *global* concordance with the data. It is not sufficient to get a *local* neat agreement on an isolated crown. The angular and the radial dependences must also be mutually consistent. This is a very powerful and significant constraint, as we will very soon find out.

The problem of fitting the data with this expression is complex, because only a limited number of experimental data points are available and a large number of parameters may enter into the considerations. Moreover, the value of this number is not known.

B. Failure of single-particle approach

The agreement between the data and the simple single-particle models is not satisfactory. In Fig. 20 we show the theoretical profiles at $Q=2.85$ Å^{-1} for various jump distances $d_i\in[1,5]$ Å. The local minima in the φ dependence along the crown at 2.85 Å^{-1} do not tally with the theoretical description. Only jumps along twofold directions are able to reproduce the strong minima observed, but they require to include a negative contribution that is constant with φ, which is unphysical. In other words, this means that the peak/valley ratios in these data are stronger than anything in the models can turn up. To quantify this, we can parametrize the data (less well) by an expression $\mathcal{C}_1+\mathcal{C}_2 S_{qel}(\mathbf{Q})$, where $\mathcal{C}_1=-6.50$, $\mathcal{C}_2=0.89$, and $S_{qel}(\mathbf{Q})$ is given by Eq. (2) for twofold jumps. These numbers are in the units used in Fig. 13.

An inspection of the models in Fig. 2 betrays quickly that we are running here into major hardship: For the three types of jumps it is quite conspicuous that moving out radially

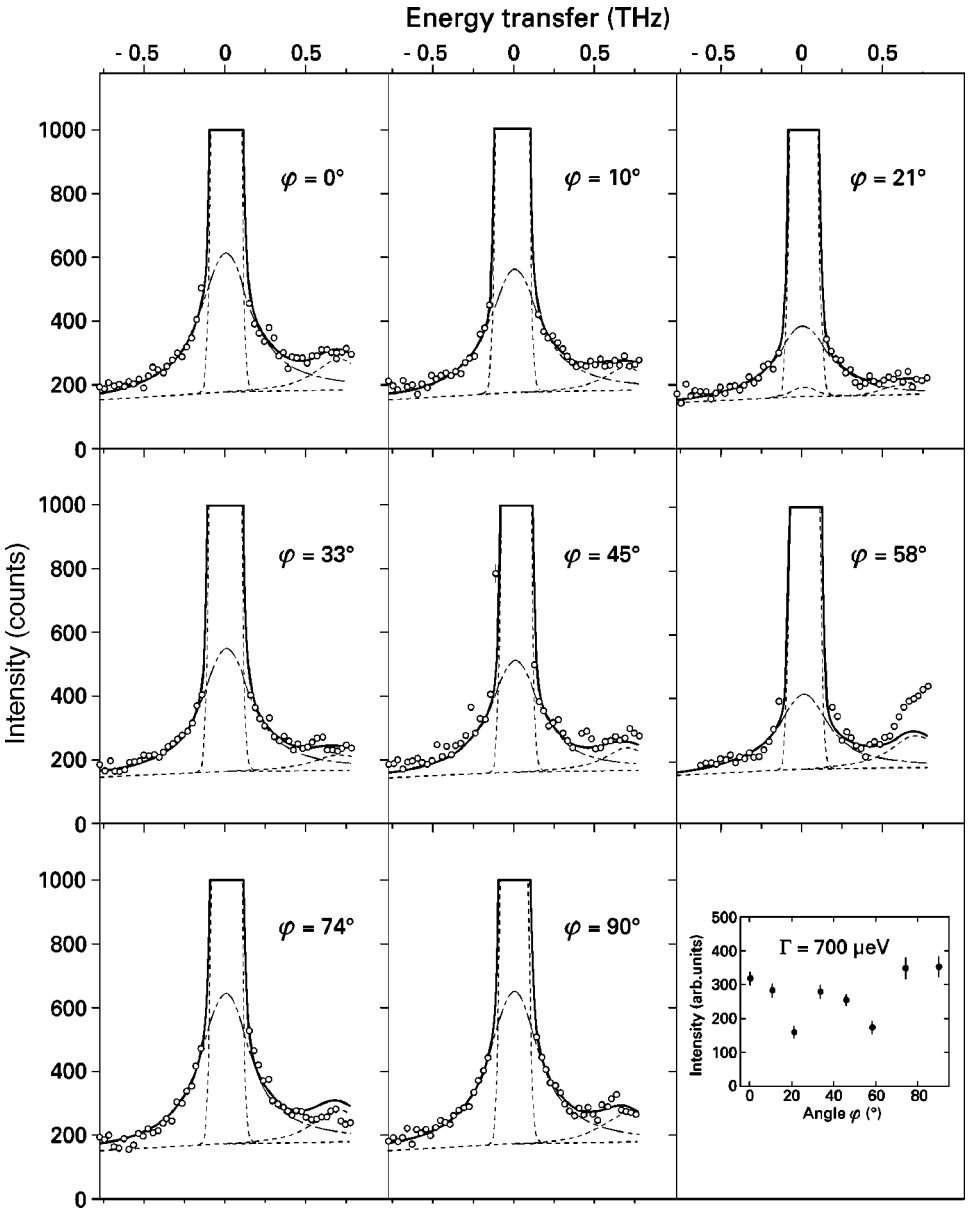

FIG. 10. Synthetic view of the nonsubtracted data on the crown at $|\mathbf{Q}|=2.85$ Å^{-1} in the the $k_f=1.97$ Å^{-1} experimental setup. These data were obtained on the small sample. The intensity profile is in concordance with the one obtained in the $k_f=1.64$ Å^{-1} setup, shown in Fig. 13.

from $Q=0$ we must encounter a first local maximum in the intensities in the form of an almost isotropic spherical shell. The reader may spot this feature on the circles corresponding to $Q=3\pi/2d$. We already pointed out the existence of these local maxima in Sec. IV. Their appearance is largely due to the high symmetry of the icosahedral group: in a given point at low **Q** there are always several symmetry axes that are not far away, such that what we observe in that point is produced by overlapping contributions from several axes. This has the effect of smoothing out the anisotropy. Only when we go further out in Q is the importance of this overlap phenomenon tempered and can we start to clearly observe some anisotropy. *The problem is now that our data do not display such an almost isotropic first local maximum in the intensi-*

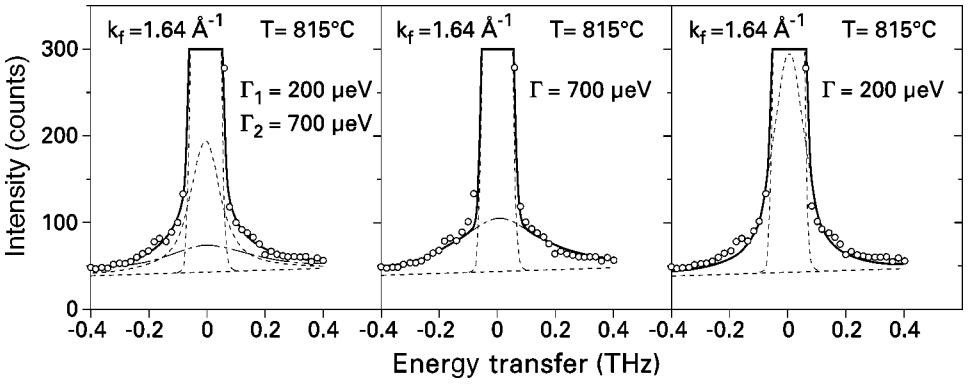

FIG. 11. Analysis of the data of the $k_f=1.64$ Å^{-1} experiment. Left: description of the data with two Lorentzians of widths $\Gamma_1=200$ μeV and $\Gamma_2=700$ μeV. Center and right: one-Lorentzian description.

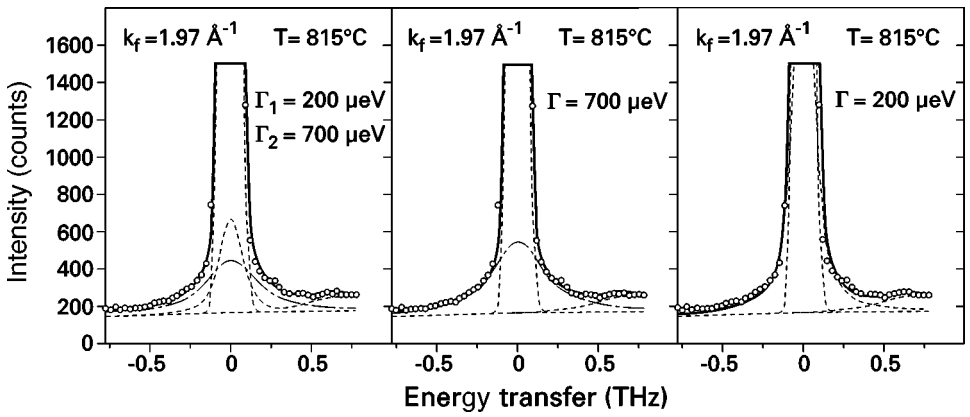

FIG. 12. Analysis of the data of the $k_f = 1.97$ Å^{-1} experiment. Left: data described with two Lorentzians of width $\Gamma_1 = 200$ μeV and $\Gamma_2 = 700$ μeV. The description with the $\Gamma_2 = 700$ μeV contribution alone (center) is of comparable quality. The description with the $\Gamma_1 = 200$ μeV contribution alone is not satisfactory.

ties. On the contrary, the first strong intensity we come across is exhibiting the most striking anisotropy in the whole data set. This feature must doom every attempt to reconcile the radial and crown dependences to failure.

We are thus getting stuck in a paradoxical situation. There is an alternative path to come to an appraisal of this circumstance. One can try to fit the data at $Q = 2.85$ Å^{-1} by brute force with an analytical model:

$$\mathcal{I}_{qel} = \mathcal{C} + \alpha_2 \mathcal{I}_2(d_2) + \alpha_3 \mathcal{I}_3(d_3) + \alpha_5 \mathcal{I}_5(d_5), \qquad (4)$$

where the indices 2, 3, and 5 now refer to jumps along the twofold, threefold, and fivefold directions. This does not work. Every hope to reproduce the single intensity profile at $Q = 2.85$ Å^{-1} by linear combinations of the three different jump models is thwarted by the fact that only models with jumps along the twofold axes can reproduce angular intensity minima, and that, as we already mentioned, these are not steep enough.

One can try to speculate as to what could be the reason for this impasse. We could, e.g., imagine that the width Γ of the quasielastic line varies with Q and that it becomes too small at lower Q values to emerge from the elastic resolution window, such that the detection of the isotropic first local maximum is missed. Such a loophole of escape from the conclusions reached above would admittedly no longer correspond to the model of Eq. (3) to the letter. But even taking this kind of freedom with scientific rigor hardly seems to hold a promise of circumventing the deadlock. The results of the time-of-flight searches[6] with an incoming wavelength of 8 Å [$\Delta E \approx 40$ μeV full width at half maximum (FWHM)] are not encouraging. We were unsuccesful in picking up the slightest indication for quasielastic scattering with a width smaller than 200 μeV.

It should be mentioned that this trouble-shooting discrepancy is not an artifact that we could put on the back of overanalyzing low-intensity data: we have found it consistently in three independent measurements at $Q = 2.85$ Å^{-1}. It is also visible to the naked eye without one having recourse to running fit procedures on the data.

C. Could the white-noise approximation be wrong?

We could also question the conceptual approach based on jump models that are merely a kind of *theme and variations* on the canonical model expressed through Eq. (1). In such models it is assumed that the jump time itself is infinitely fast. The relaxation times are average residence times. Hence, such models do not offer a description of the particle on its way in between the two minima of the double-well potential. It is assumed that such information will not be reflected in the data if the jumps are occurring on very short time scales. This is called the white-noise approximation. This conceptual drawback has been challenged by Michel and his co-workers[80] who developed a much more sophisticated approach using an elegant formalism of symmetry-adapted functions. The ensuing mathematical expressions for the intensities are rather intractable. We have seen that in the assisted situation the atom sees a very low potential energy barrier. Could it be that the hopping atom has comparable probabilities to be probed everywhere within a tube that links the two sites, such that our data would contain information that corresponds to snapshots of the scurrying particle on its way in between? If this were true, the situation would be pretty hopeless, since it would ask for the knowledge of a detailed picture of the atomic potential in the assisted state in order to permit further progress. Guessing what these potentials might be introduces in a sense a continuum of parameters, viz., the value $V(s)$ of the potential at each point with spatial coordinate s inside the tube. Given the low potential barriers that are associated with the assisted state, we could attempt a flat potential. But a model based on this idea yields a **Q** dependence that is even less satisfactory than the models we have developed so far. It displays very strong axial anisotropy with radially running ridges and valleys that seem to extend indefinitely to high Q values. Fortunately, it can be said that the *practical approach* embodied by the theme and variations of Eq. (1) has consistently proved satisfactory within the realm of quasielastic neutron scattering, even in the cases of very fast motion such as rotational diffusion of molecules. We dismiss thus the possibility of a failure of the white-noise approximation based on Eq. (1) on two grounds, viz., likelihood and practical feasibility, the latter criterion being admittedly not a scientific one.

D. Parametrization that works

If it proves so difficult to elicit the anisotropy observed on the basis of the model crystallized in Eq. (4), despite the fact that it contains so many adjustable parameters, it must mean that our data contain some very strong piece of information that addresses a crucial point that hitherto has eluded our awareness. In our unsuccessful trials to fit the data, we

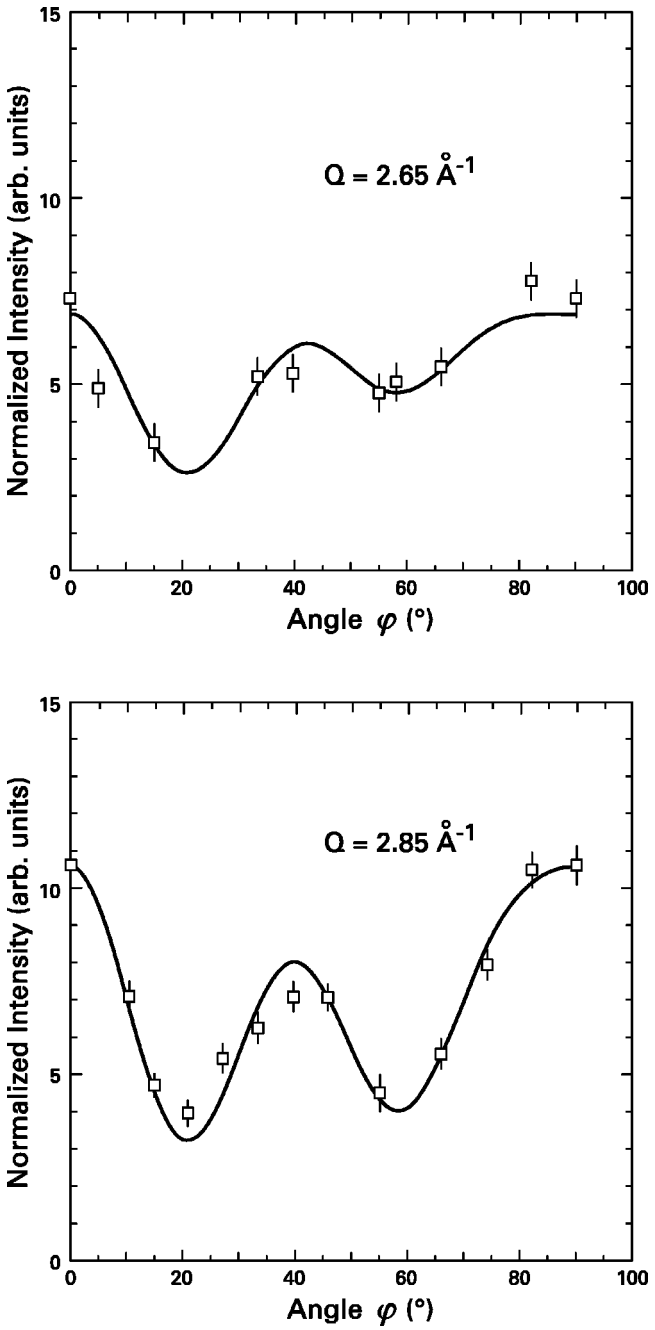

FIG. 13. Experimental intensities from the fits of the $k_f = 1.64$ Å^{-1} measurements on the crowns at $|\mathbf{Q}| = 2.85$ Å^{-1} (top) and $|\mathbf{Q}| = 2.65$ Å^{-1} (bottom). The fits are made on the nonsubtracted data ($k_f = 1.64$ Å^{-1}, large sample) with only one Lorentzian with a width $\Gamma = 400$ μeV. The data are directly compared to the ''unreasonable'' model fit of Eq. (5).

stumbled accidentally (by error) onto a very strange observation: The data at $Q = 2.85$ Å^{-1} are extremely well fitted by an expression

$$C_1 \sum_{i=1}^{10} \frac{1}{2}[1+\cos(\mathbf{Q}\cdot C_2\mathbf{e}_i^{(3)})] + C_3, \tag{5}$$

where $\mathbf{e}_i^{(3)}$ are the ten unit vectors along the threefold directions and $C_2 = 3.83$ Å. This is shown in Fig. 13. This means that the quasielastic intensity profile is *inverted* and follows the *elastic* structure factor $S_{el}(\mathbf{Q})$ of a model for threefold jumps rather than the *quasielastic* structure factor $S_{qel}(\mathbf{Q}) = 1 - S_{el}(\mathbf{Q})$. (The reader may remember that we pointed out that the quasielastic and elastic structure factors obey a sum rule.) It should be emphasized that this is an alienating if not absurd finding: a $\frac{1}{2}[1+\cos(\mathbf{Q}\cdot\mathbf{d})]$ dependence for the quasielastic intensity is most unusual. We refer the reader to the various jump models for a particle jumping between N equivalent sites on a regular polygon treated by Bée,[51] and summarized in Table 6.2. on p. 200 of his monograph. We also refer the reader to the model for jumps between two nonequivalent sites, treated in the same work on p. 191. Finally, we refer the reader to the expressions derived within the framework of our assistance model summarized in Tables I and II on page 1687 of Ref. 74. Hence, just like the T behavior, the Q behavior of atomic hopping in QCs is doing the opposite of what it ought to do. Can we figure out why?

E. Elser's escapement model

We might consider the following idea that in its spirit is reminiscent of a model conceived of by Elser.[38] It raises the possibility of an interesting link between the **Q** and the T dependence. In this model we assume that the scene of the dynamics is a two-winged structure with a more or less dumbbell-shaped silhouette. The two wings are equivalent configurations that are interlocked. If one wing is locked, the other one is unlocked and vice versa. The system flips between the two situations with a long relaxation time. An atom will be allowed to jump quickly during the time that its surroundings define the unlocked part of the structure. But if the balance is tipped and the atom finds itself within the locked part, then the jumps are frozen. The idea would be that the elastic structure factor corresponding to the average dumbbell geometry could modulate the quasielastic structure factor of the dynamics. In Elser's model each wing is actually a copy of our model of twofold jumps we briefly depicted in Sec. IV, and spelled out in more detail in Ref. 75. Elser mused on a delightful analogy between this interlocked situation and the functioning of a lever escapement in a wrist watch, a clever mechanical device that was originally invented by the Dutch physicist Christiaan Huygens in the 17th century.[81] But of course Elser's model is far too complicated to be calculated analytically. Before going headlong into a tedious numerical elaboration of it we first should try to validate the idea that underpins it on a downsized model that captures its essence.

This simplified model can be described as follows (see Fig. 21). We consider three double-well potentials AB, CD, and EF, each housing one particle. The jump vectors **d** of two of the double wells AB and EF are equipollent and aligned along the opposite edges of a rectangle. The third double well CD has a jump vector $\mathbf{v} \perp \mathbf{d}$. This double well CD is positioned in the center of the rectangle. The length v is of course shorter than the distance between the two double wells with equipollent separation vectors **d**. The escapement that controls the swing of the pendulum is here the particle in the double well CD: it blocks the jumps in the double well it is closer to. The result of this (cumbersome) model calculation is given in the Appendix B. The bottom line is that our

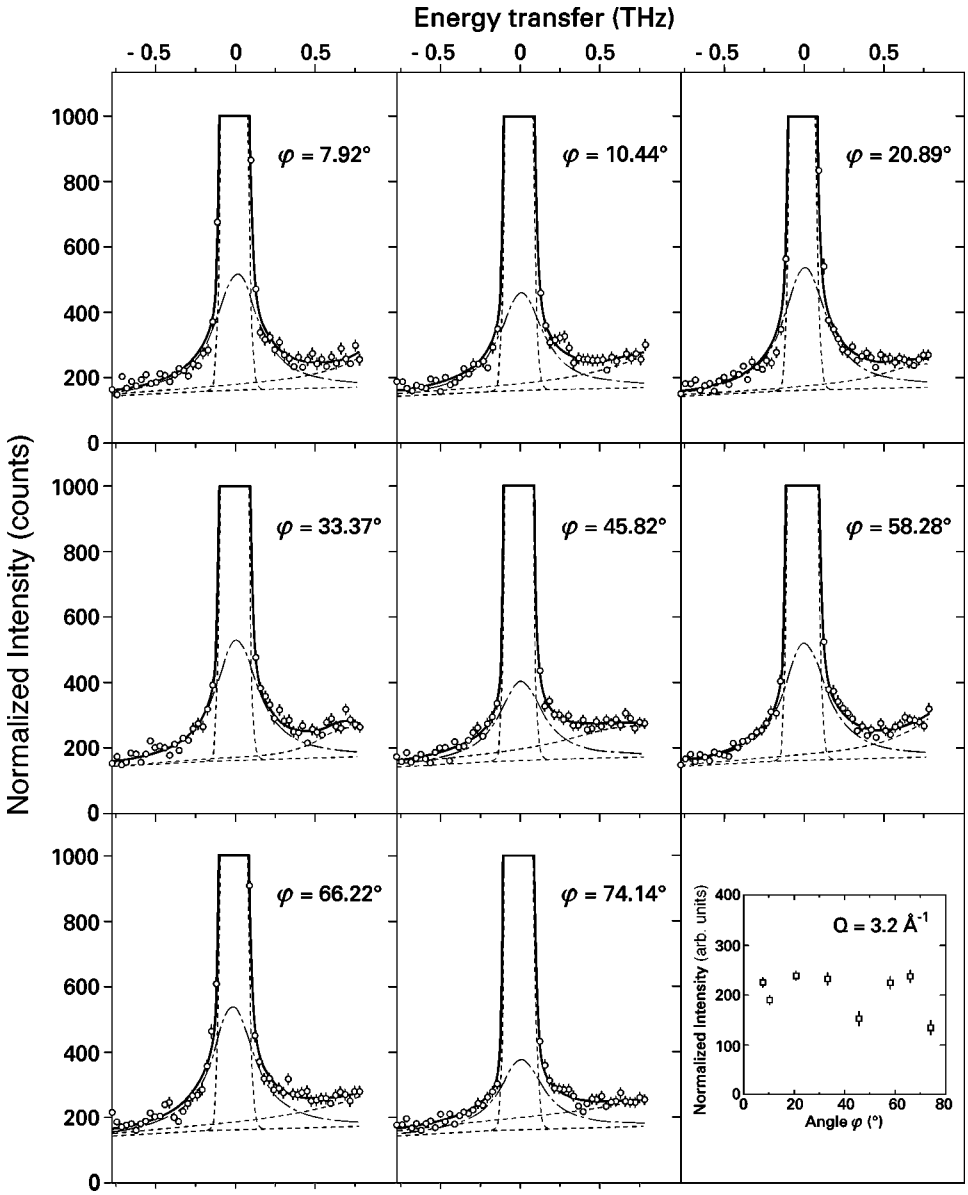

FIG. 14. Panorama of the non-subtracted data on the crown at $|\mathbf{Q}|=3.2$ Å^{-1} in the the $k_f=1.97$ Å^{-1} experimental setup. These data were obtained on the small sample.

efforts do not pay off: We obtain $\frac{1}{2}[1-\cos(\mathbf{Q}\cdot\mathbf{v})]$ dependences. Other incentives with a similar flavor came to the same results. In fact our aim was to factorize the structure factor into a product of terms that are related to the characteristic distances involved in the slow and the fast dynamics. But this factorization takes place in the time domain rather than in the space domain. The jump matrix is indeed a Kronecker tensor product of two simpler jump matrices. But the Fourier transforms of two configurations just add up; they do not multiply. Apparently we have not stretched our imagination far enough and we are still missing the point.

F. Correlated jumps

Our failure to seize the anomalous **Q** depencence of our data within an approach based on Elser's model highlights the fact that any temporal variation of the neutron-scattering contrast between two sites X and Y produced by an atom jumping between them ends up being tagged by a $\frac{1}{2}\{1-\cos[\mathbf{Q}\cdot(\mathbf{r}_X-\mathbf{r}_Y)]\}$ dependence. We finally reach the conclusion that if we want to tease out a $\frac{1}{2}[1+\cos(\mathbf{Q}\cdot\mathbf{d})]$ factor, we must tailor our jump models in such a way that despite the dynamics a separation vector **d** remains preserved within the system with an unchanged neutron-scattering contrast. In all the models we tried up to now, when an atom jumps between two sites, the neutron-scattering contrast between the two sites is inverted by the jump. This leads to a π flip of its phase and is eventually responsible for the appearance of the nagging minus signs that kept popping up so stubbornly in front of the cosines within all the quasielastic structure factors of the models we considered. We can only preserve the phase of a contrast labeling a given separation vector if we admit that two (or more) atoms are jumping *simultaneously*, such that $\mathbf{d}=\mathbf{r}_X-\mathbf{r}_Y$ can be preserved with the same neutron-scattering contrast under the new form $\mathbf{d}=\mathbf{r}_{X'}-\mathbf{r}_{Y'}$. The simplest realization of this idea would be that two atoms jump in concert with equipollent jump vectors ($X\rightarrow X'$ and $Y\rightarrow Y'$). We can appreciate that this will do the right thing by designing an almost trivial model. We imagine two double wells AB and CD with equipollent separation vectors $\mathbf{AB}=\mathbf{CD}=\mathbf{d}$, again aligned along the opposite edges of a rectangle $ABCD$. The two remaining edges of the rect-

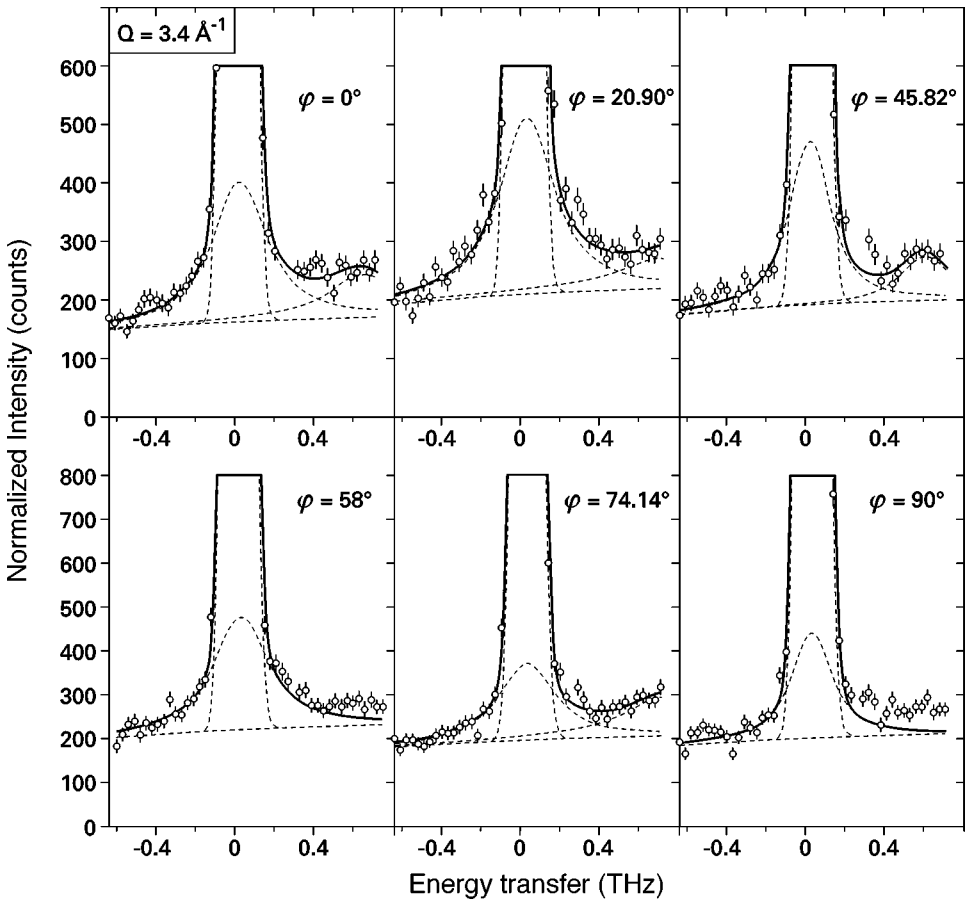

FIG. 15. Panoramic view of the nonsubtracted data on the crown at $|\mathbf{Q}|=3.4$ Å^{-1} in the $k_f=1.97$ Å^{-1} experimental setup. These data were obtained on the small sample. The phonon background hinders the data analysis.

angle define the perpendicular vector $\mathbf{s}=\mathbf{AC}=\mathbf{BD}$. When we assume that the two particles jump in phase with a relaxation time τ, we find (see Appendix C):

$$S(\mathbf{Q},\omega)=2\sigma[1+\cos(\mathbf{Q}\cdot\mathbf{s})]\left[\frac{1}{2}[1+\cos(\mathbf{Q}\cdot\mathbf{d})]\delta(\omega)+\frac{1}{2}[1-\cos(\mathbf{Q}\cdot\mathbf{d})]\Lambda(\omega)\right], \quad (6)$$

where

$$\Lambda(\omega)=\frac{1}{\pi}\frac{\Gamma}{\Gamma^2+(\hbar\omega)^2}$$

as usual and σ is the cross section of the two jumping atoms. We may call this an exhilarating result. It defeats Elser's model and everything else we expected based on our common sense. In fact, an atomic jump is a stochastic process. It is, e.g., triggered by the random thermal fluctuations of the environment of the atom. We therefore *a priori* never considered the possibility of a choreography of simultaneous jumps. As Elser[38] we assumed that while a tile flip in a real structural model would correspond to several jumps, these would not occur simultaneously. The basic process in a real QCs would thus not be a tile flip, but rather an atomic jump. We thus implicitly rejected the possibility of several kinds of phason dynamics by combining elementary jumps into various levels of hierachy, building phasons, superphasons, etc, although a number of scientists interpreted a model by Zeger and Trebin[82] this way. One should rather be inclined to dismiss such a paradigm highhandedly. Now our data seem to suggest that it has to be taken seriously.

Perhaps we should emphasize the impossibility to derive $[1+\cos(\mathbf{Q}\cdot\mathbf{s})]$ dependences from a model with one-particle jumps, even within the framework of a formulation that allows for coherent quasielastic signals: In the relevant algebra intermediate structure factors of the form $S_{jk}(\mathbf{Q},t)=\langle\mathcal{F}_j(\mathbf{Q},t)\mathcal{F}_k^*(\mathbf{Q},0)\rangle$ arise. Here $\mathcal{F}_j(\mathbf{Q},t)$ is the Fourier transform of a configuration j at time t. One might anticipate that if in the transition from configuration j to configuration k many atomic positions $\mathbf{r}_n$, $\mathbf{r}_m$, . . . remain the same, then $S_{jk}(\mathbf{Q},t)$ could lead to many terms of the type $1+\cos[\mathbf{Q}\cdot(\mathbf{r}_n-\mathbf{r}_m)]$. The snag is that these contributions vanish in the final result. We have given a quite general proof in Ref. 83 that the correlations between unaltered site occupations remain silent in the dynamical response for coherent models. The reader can get an inkling of the gist of this idea from a handwaving argument developed in the Appendix D. Eventually this is also the culprit of the breakdown of our attempt based on Elser's model.

G. Final remarks

Both at $Q=2.85$ Å^{-1} and at $Q=2.65$ Å^{-1} the trial function of Eq. (5) works well with a value $s=C_2=3.83$ Å. The parameter C_1 replaces the ''prefactor'' $\frac{1}{2}[1-\cos(\mathbf{Q}\cdot\mathbf{d})]$, which is warranted by the reasonable assumption that d is much smaller than s, such that its angular dependence is still isotropic at these Q values. The quality of the fits is not significantly improved by including the global adjustable

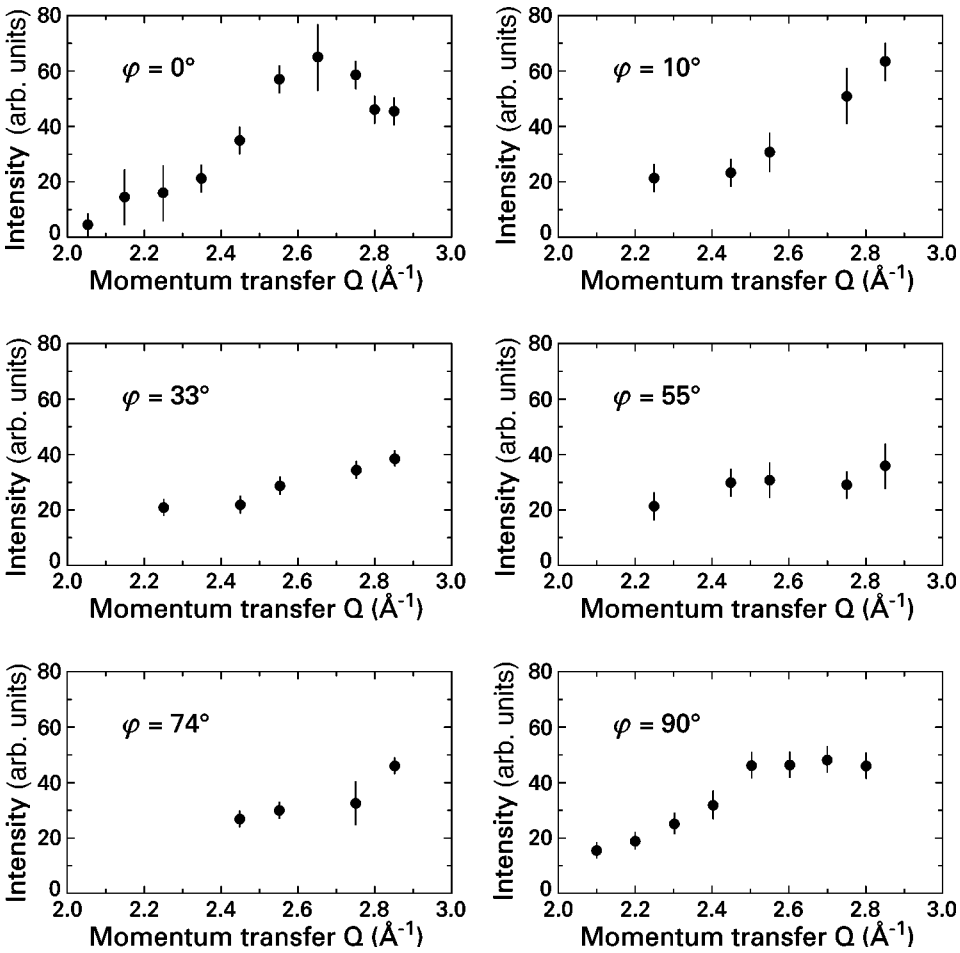

FIG. 16. Radial intensity profiles in the $k_f = 1.64$ Å^{-1} setting of the spectrometer: only the data along the (twofold) Q_x axis reach a local maximum within the Q range available.

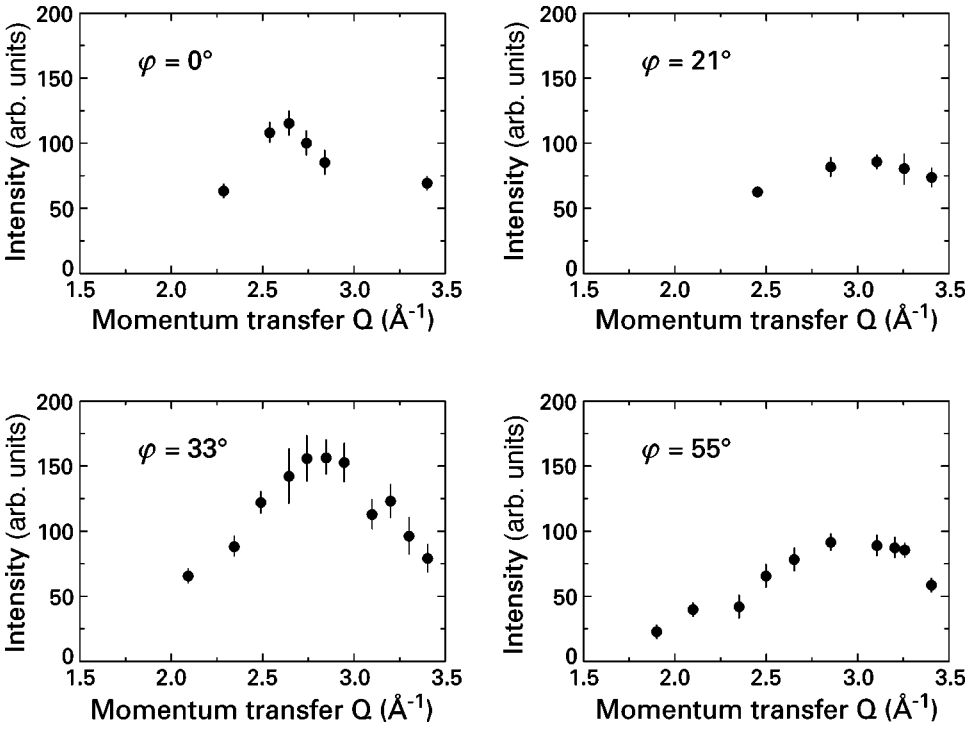

FIG. 17. Radial intensity profiles in the $k_f = 1.97$ Å^{-1} geometry of the spectrometer: in all cases a local maximum is reached within the Q range available.

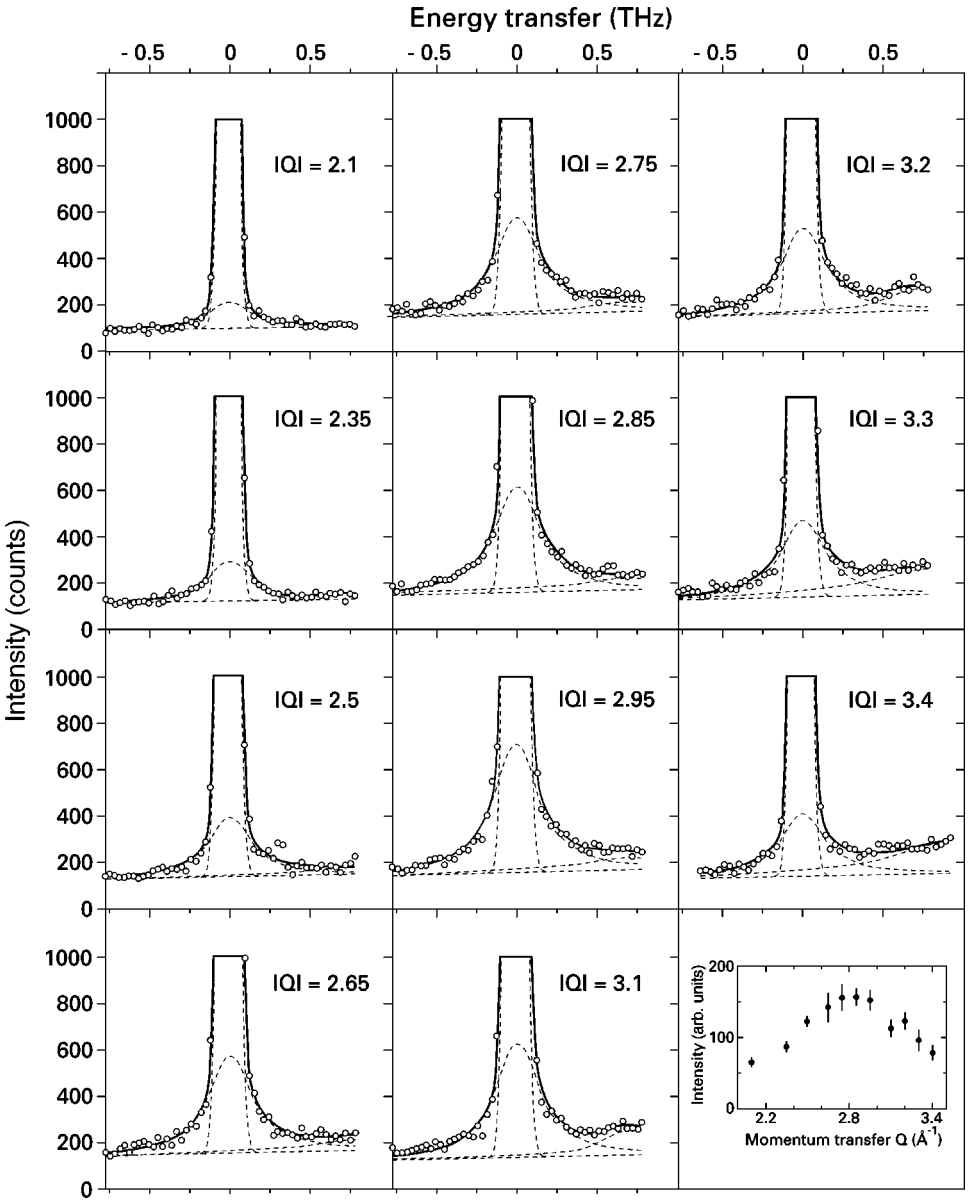

FIG. 18. High-temperature raw data measured along the axis at $\varphi = 33°$ between 2.1 and 3.4 Å^{-1}.

constant C_3. A constant contribution could have arisen from another jump over a short distance.

At this point our grappling with the interpretation of the data must grind to a halt. The radial profiles at $k_f = 1.64$ Å^{-1} could be determined by $\Sigma_{i=1}^{10} \frac{1}{2}[1+\cos(\mathbf{Q} \cdot C_2 \mathbf{e}_i^{(3)})]$, provided $\frac{1}{2}[1-\cos(\mathbf{Q}\cdot\mathbf{d})]$ behaves approximately as a constant. But this behavior does not reproduce the first intensity maximum observed on the Q_x axis both in the $k_f = 1.64$ Å^{-1} and the $k_f = 1.97$ Å^{-1} data.

Furthermore, if we extrapolate the trial funcion of Eq. (5) to $Q = 3.2$ Å^{-1}, we see that it still should exhibit minima on the fivefold and threefold axes. This is not so in the data. The general tendency is actually inverted: We are encountering now maxima on the fivefold and threefold axes. In fact, we can fit the crown at 3.2 Å^{-1} again with a normal model consisting of a constant and the function of Eq. (2) by assuming threefold jumps over a distance of 3.4 Å. This rather abrupt change in the φ dependence of the intensities with Q is a renewal of the difficulties. We explored several lines of thought in our attempts to face this difficulty.

(1) The further we go out in Q space the more characteristic distances will contribute to the signal. It is well known from the structural models that we can expect a large number of such distances. In the long-wavelength limit we were so

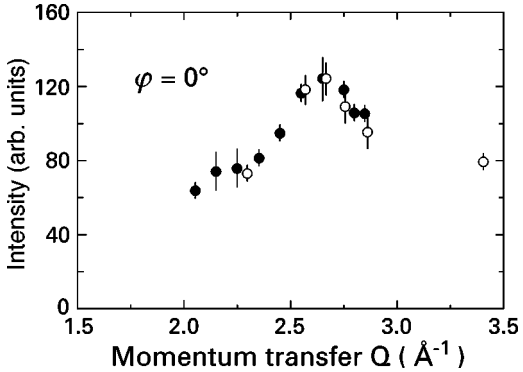

FIG. 19. Radial dependence of the intensities from the $k_f = 1.64$ Å^{-1} (solid circles) and $k_f = 1.97$ Å^{-1} (open circles) measurements on the twofold Q_x axis. The intensities have been normalized with respect to each other.

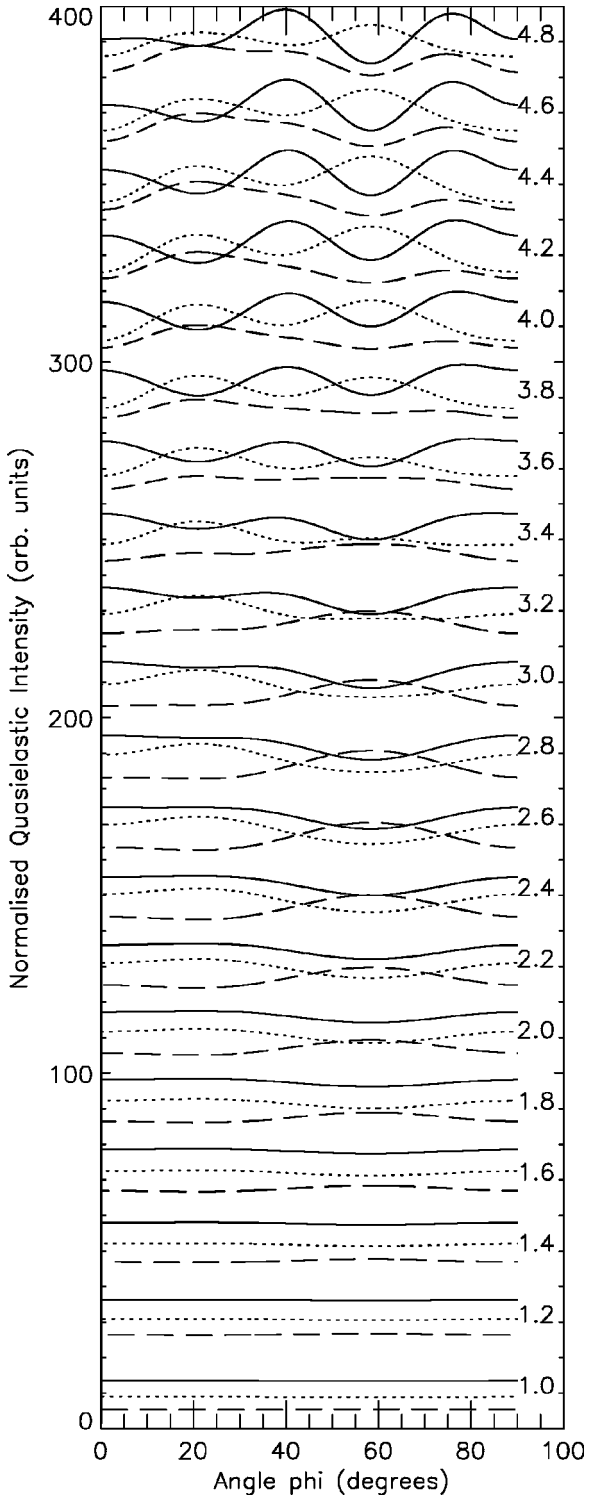

FIG. 20. Calculated intensities [Eq. (2)] on the crown at $Q_0 = 2.85$ Å^{-1} for jump distances $d_i \in [1,5]$ Å^{-1} as labeled on the right hand side of the figure. The base lines have been shifted by multiples of 20 in order to condense the various results into one single figure. Jumps along the twofold (solid line), threefold (dotted line), and fivefold (dashed line) axes are each time shown. These curves correspond directly to circular sections through the contour plots of Fig. 2. The angle φ is measured from the Q_x axis. The recipe to read the results for other (Q,d) combinations from the figure follows from the observation that the only relevant parameter in the models is the aggregate Qd.

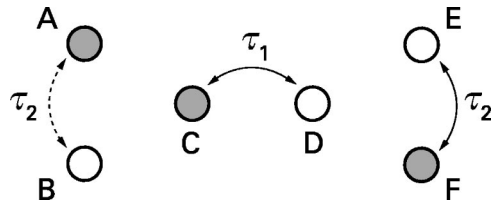

FIG. 21. Simplified model permitting one to catch the gist of the escapement mechanism proposed by Elser. The atom in *A* is blocked due to the presence of the atom in *C*, while the atom in *F* is free to leap to and fro *E* with relaxation time τ_2. A jump of the atom from *C* to *D* (with relaxation time τ_1) tips the balance, by blocking atom *F* and unlocking atom *A*. The double well *CD* fulfills the role of the escapement. In the full-fledged model both double wells *AB* and *EF* must be replaced by a dodecahedron containing seven atoms. Despite its profusive detail, this model is not able to explain the intensities shown in Fig. 13.

fortunate to be able to discern the isolated Q dependence of one such intrinsic distance. From 3.2 Å^{-1} onwards there could be more than one contribution present in the data. We must then assume that there is a strong contribution from jumps along threefold directions in order to turn the minima into maxima as observed. But from Fig. 20 it may be noted that to obtain pronounced maxima of this kind implies again a rather large jump distance. As the model functions vary rather smoothly with $\mathbf{Q}$ it is hard to see how this contribution that dominates at $Q = 3.2$ Å^{-1} can be entirely absent at 2.85 Å^{-1}. Even if it were compensated by the anomalous contribution expressed by Eq. (5), there should have been a part $\mathcal{C}_3 \neq 0$ at $Q = 2.85$ Å^{-1}, which is barely the case.

(2) Another possibility could be that the factor $1 - \cos(\mathbf{Q}\cdot\mathbf{d})$ in Eq. (6) starts to deviate significantly from a constant at higher Q values. For each of the jumps with vector $\mathbf{d}_i$ there must be an associated threefold direction $\mathbf{s}_i$. There is thus a correlation between $\mathbf{s}_i$ and $\mathbf{d}_i$ which must be carried through by the symmetry operations of the icosahedral group. Equation (5) is then no longer a good approximation for the exact expression which rather should read

$$S(\mathbf{Q},\omega) = 2\sigma \sum_{i=1}^{10} [1+\cos(\mathbf{Q}\cdot\mathbf{s}_i)]\left[\frac{1}{2}[1+\cos(\mathbf{Q}\cdot\mathbf{d}_i)]\delta(\omega) + \frac{1}{2}[1-\cos(\mathbf{Q}\cdot\mathbf{d}_i)]\Lambda(\omega)\right]. \quad (7)$$

If we assume that the vectors $\mathbf{d}_i$ are along a symmetry direction, then there are 60 combinations to be explored, with an unknown jump distance d. Even if we were to find a magic combination that works, it would look *ad hoc* in view of the limited number of data to validate it. But it does not look plausible to us that any of the sums of the kind of Eq. (7) could mimick the effect of inverting the signs in front of the cosines in the terms $1+\cos(\mathbf{Q}\cdot\mathbf{s}_i)$. In fact, all these terms are weigthed by positive numbers $[1-\cos(\mathbf{Q}\cdot\mathbf{d}_i)]$.

(3) The correlations are even more complex. But we fear that dreaming up more complicated models must be a losing battle. Our data are not good enough for a more sophisticated approach and the number of possibilities is almost unlimited. Given the basic smoothness of the jump models, the sheer

change in the φ dependence with Q observed in our data should prove an abiding hotbed of difficulties.

(4) Both the behavior at $Q=2.85$ Å^{-1} and at $Q=3.2$ Å^{-1} indicate the presence of threefold jumps. But at 2.65 Å^{-1} the signal is collective, while at 3.2 Å^{-1} we have the signature of individual behavior. It seems to us that the most plausible explanation of the data would be that there is a *cross over* between two regimes, somewhat in the spirit of the Aubry transition between continuous and discontinuous phason modes in the Frenkel-Kantorova[84] model or some other models of composite incommensurate structures.[85] Such transitions are indeed abrupt: they depend on a critical value of a parameter in the model. This is definitely a fascinating possibility, but we have no clue as to how one could substantiate it any further within the current stage of theoretical knowledge. We hope that our experimental results may constitute a strong motivation to dig further into such models in order to unfold their delimitations.

At this point we must thus resign from trying to obtain a more detailed understanding of our data. This is a negative result. But rather than as a catastrophe it must be considered as the first hint that something unexpected is going on. Hence, it transpires that due to correlations and to a large number of jumps the situation becomes so blurred that only the largest characteristic distance in the system can be extracted from the data. This relies on the possibility of isolating it in a small-Q limit where all other contributions are still negligible.

IX. CONCLUSION

The impossibility of reproducing the experimental behavior observed theoretically by any single-particle model of the type embodied by Eqs. (2) and (3) shows that phasons in QCs do not occur as isolated jumps, but as strongly correlated sets of jumps.

It is remarkable that in both Al-Cu-Fe and in Al-Mn-Pd 3.8 Å shows up as an important distance. This suggests that the Al-Cu-Fe result could also be due to some collective effect.

The model by Zeger and Trebin is not the only one that predicts simultaneous jumps. Beraha *et al.* observed a structural transition between the ξ and ξ' phases in Al-Mn-Pd by electron microscopy. The transformation gives the visual impression of collective jumps of whole ''clusters'' over a distance of 4.8 Å. They propose a microscopic mechanism based on Mn jumps of 2.82 Å along fivefold directions, Pd jumps over 2.96 Å along twofold directions, Al jumps over 2.96 Å and 1.83 Å along twofold directions, and finally Al jumps over 2.57 Å along threefold directions. The motion of the atomic surface in hyperspace that produces Mn jumps is such that four Mn atoms jump *simultaneously*. We must also quote here a suggestion by Trebin[86] who has evoked an image of a wave of collective jumps as an elastic response of the quasiperiodic medium to a periodic external source of deformation, e.g., in a vibrating-reed experiment. Such an elastic response must then be governed by the phason elastic constants. We must pay a tribute here to these authors for their perspicacity.

Finally, it should be mentioned that there is an interesting link between our data and the symmetry of the thermal diffuse scattering data. Capitán *et al.*[87] have demonstrated that the phason elasticity that explains the intensity contours around the Bragg peaks corresponds to deformation along the threefold directions.

ACKNOWLEDGMENTS

The authors would like to thank Philippe Boutrouille and Patrick Baroni for technical assistance during the experiments. One of us (G.C.) would like to express his gratitude to Wilhelmina Bouws.

APPENDIX A: ARE PHASON JUMPS PRODUCED BY VACANCIES?

Recently[68] Dubois *et al.* commented on our work.[1,2,5,6] They observed quasielastic scattering[88] in a $B2$ phase $Al_{50}Cu_{35}Ni_{15}$. The authors used this to affirm that it would prove that *fast atomic hopping is nothing special for QCs, and occurs more commonly provided sufficient vacancies are available.*

In order to reach such conclusions Dubois *et al.* tacitly introduce a number of assumptions: (1) viz., that the *structural* vacancies in the $B2$ phase are responsible for the fast hopping observed. If vacancies do play a part at all in hopping within the $B2$ phase, then one should first try to elucidate of which type they are, i.e., if they are *structural* or *thermal* vacancies. But whatever species these vacancies are of, if the existence of phason jumps in QCs were just due the existence of vacancies, then this would imply an altogether different temperature behavior of the quasielastic signal than found in QCs where the hopping is assisted rather than vacancy mediated. This remark shows that they also foster the assumption (2) that there exists only one universal (vacancy-mediated) mechanism for hopping in an alloy. It is also clearly taken for granted (3) that there would be a large number of structural vacancies in a QC. But there is no incentive in the form of experimental evidence that makes it worth our while pondering seriously over such an ansatz.[89]

In order to prove with mathematical rigor that these claims are wrong, it would be necessary to pin down the number of vacancies in a QC, which is an extremely hard and ungratifying job. Density measurements on a single crystal are beset with large uncertainties due to the presence of large facetted voids of dodecahedral shape.[90] And positron-annihilation experiments are not really reliable. It should, however, suffice to reject the claims firmly based on the millenia-old principle *actori incumbit probatio*. Nevertheless, we will do some more by listing below a number of arguments that tend to discredit this claim.

For certain stoichiometries the archetypal $B2$ phase AlNi can harbor up to 12% of *structural* vacancies at room temperature. This figure obtained by a comparison of the lattice parameter and density data[91] can be assessed also by Mössbauer spectroscopy in the case of CoGa:[92] the presence of vacancies is evidenced by a strong quadrupole-shifted additional component; i.e., one can distinguish the population of sites with a complete neighborhood from the population of sites with a vacancy in its neighborhood.[93] At room temperature the Mössbauer data underestimate the vacancy concentration. This deficit is explained as an effect of vacancy clus-

tering. But at high temperature the clusters dissociate and the Mössbauer estimate of their concentration becomes accurate. Similar spectroscopic data for QCs (e.g., within the Al-Cu-Fe system) do not suggest the presence of a large structural-vacancy concentration.[94] The presence of vacancies must lead to a larger electric-field gradient (EFG) than in the situation when there is no vacancy in the nearest-neighbor shell. The fact that the EFG in Al-Cu-Fe decreases smoothly with T shows that there is motional narrowing, but no other ''site'' or phase appearing.[4] An Fe atom with a vacancy as nearest neighbor would be an additional site, very different from one with a full shell. Some small number of thermal vacancies together with the high-temperature diffusion should provide enough atomic flux to form the microscopic voids seen by a number of groups.[90] There is no need for a large number of (structural) vacancies. In fact there is only one population of sites in the sample. This population has a large distribution, which becomes *narrower* at high temperature. It is clear that in a QC the ditribution of sites with a vacancy in their neighborhood could be much less sharp than in a $B2$ compound but it would be far fetched to claim that a distribution of a few percent of such sites would go unnoticed. (Positron-annihilation studies have yielded an estimate that the vacancy concentration at room temperature in Al-Cu-Fe is of the order of 8 ppm, but such data are not always reliable[95]).

The absence of a large concentration of structural vacancies in QCs is further corroborated by the totally disparate outlook of the existence domains of $B2$ phases and QCs. They bear no ressemblance whatsoever and have very different extents. Whereas the $B2$ structure is very insensitive to atomic composition as indicated by a sizable stability range within the phase diagram,[91] QCs on the contrary are extremely sensitive to it.[62] A variation of 1% in composition is sufficient to render the QC structure unstable. In the $B2$ phases this stability of the structure in the Al-rich phases is obtained by just leaving Ni sites unoccupied (i.e., by building in structural vacancies), while in the Ni-rich phases it is obtained by introducing antisite atoms.[96] The intensity of the atomic hopping in QCs is not seen to be different in a powder and in a bulk sample, despite the much larger surface present in the former. This means that the occurrence of a large number of dodecahedral voids seen by x-ray topography[90] in Czochralski-grown samples is not sufficient an indication of the existence of a large number of vacancies. Structural studies on icosahedral phases are claimed to yield the positions of 95% of the atoms, but do not invoke a role for vacancies.[19,38,39]

If we were to believe the vacancy scenario, then the fact that it takes an exceptionally large concentration of structural vacancies to match the quality of the results obtained in a QC, where the number of vacancies is several orders of magnitude lower, can only underline that indeed something special is going on in the QC. But it is probably wise to refrain from paraphrasing in such slogan-oriented terms the scientific mission that has fallen to our share: The true objective we fixed ourselves from the outset can only be the elucidation of the phason concept in QCs.

APPENDIX B: MODEL CALCULATION

The dynamical structure factor of the the downsized escapement model is calculated by recasting the model in terms of configurations, following the method spelled out in Ref. 83. There are eight configurations, linked by the following scheme of transitions:

$$\begin{array}{ccccc} BCF & \overset{\tau_1}{\leftrightarrow} & BDF & \overset{\tau_2}{\leftrightarrow} & ADF \overset{\tau_1}{\leftrightarrow} ACF \\ \updownarrow \tau_2 & & & & \updownarrow \tau_2 \\ BCE & \overset{\tau_1}{\leftrightarrow} & BDE & \overset{\tau_2}{\leftrightarrow} & ADE \overset{\tau_1}{\leftrightarrow} ACE \end{array}$$

where the symbol XYZ denotes that the postions X, Y, and Z are occupied while the other ones are empty. Noting $\gamma_i = 1/\tau_i$, the corresponding jump matrix $\mathbf{M}$ can be written as

$$\begin{pmatrix} -(\gamma_1+\gamma_2) & \gamma_1 & 0 & 0 & 0 & 0 & 0 & \gamma_2 \\ \gamma_1 & -(\gamma_1+\gamma_2) & \gamma_2 & 0 & 0 & 0 & 0 & 0 \\ 0 & \gamma_2 & -(\gamma_1+\gamma_2) & \gamma_1 & 0 & 0 & 0 & 0 \\ 0 & 0 & \gamma_1 & -(\gamma_1+\gamma_2) & \gamma_2 & 0 & 0 & 0 \\ 0 & 0 & 0 & \gamma_2 & -(\gamma_1+\gamma_2) & \gamma_1 & 0 & 0 \\ 0 & 0 & 0 & 0 & \gamma_1 & -(\gamma_1+\gamma_2) & \gamma_2 & 0 \\ 0 & 0 & 0 & 0 & 0 & \gamma_2 & -(\gamma_1+\gamma_2) & \gamma_1 \\ \gamma_2 & 0 & 0 & 0 & 0 & 0 & \gamma_1 & -(\gamma_1+\gamma_2) \end{pmatrix}. \tag{B1}$$

We introduce the notation $\gamma_1/\sqrt{\gamma_1^2+\gamma_2^2} = \cos\alpha$, $\gamma_2/\sqrt{\gamma_1^2+\gamma_2^2} = \sin\alpha$, and $\sqrt{\gamma_1^2+\gamma_2^2} = X$. The jump matrix can be diagonalized by observing that every second configuration connects the same way to its neighbors. This is thus a problem with ''translational symmetry.'' The system has the same topology as a phonon problem for a linear diatomic chain, with cyclic boundary conditions and four unit cells. We can map our jump problem onto this phonon problem. The latter can be solved by using the Bloch theorem. We must thus propose eigenfunctions

TABLE III. Components of $S(\mathbf{Q},\omega)$ in an escapement model.

Spectral function	Weight	Structure factor
$\delta(\omega)$	$\frac{1}{2}\sigma_f$	$\cos[\mathbf{Q}\cdot(\mathbf{r}_A-\mathbf{r}_F)]+\cos[\mathbf{Q}\cdot(\mathbf{r}_B-\mathbf{r}_F)]$ $+\cos[\mathbf{Q}\cdot(\mathbf{r}_E-\mathbf{r}_F)]+\cos[\mathbf{Q}\cdot(\mathbf{r}_A-\mathbf{r}_E)]$ $+\cos[\mathbf{Q}\cdot(\mathbf{r}_B-\mathbf{r}_E)]+\cos[\mathbf{Q}\cdot(\mathbf{r}_A-\mathbf{r}_B)]+2$
	$\frac{1}{2}\sigma_s$	$1+\cos[\mathbf{Q}\cdot(\mathbf{r}_C-\mathbf{r}_D)]$
	$\frac{1}{2}\sqrt{\sigma_f\sigma_s}$	$\cos[\mathbf{Q}\cdot(\mathbf{r}_A-\mathbf{r}_C)]+\cos[\mathbf{Q}\cdot(\mathbf{r}_B-\mathbf{r}_C)]$ $+\cos[\mathbf{Q}\cdot(\mathbf{r}_A-\mathbf{r}_D)]+\cos[\mathbf{Q}\cdot(\mathbf{r}_B-\mathbf{r}_D)]$ $+\cos[\mathbf{Q}\cdot(\mathbf{r}_C-\mathbf{r}_E)]+\cos[\mathbf{Q}\cdot(\mathbf{r}_D-\mathbf{r}_E)]$ $+\cos[\mathbf{Q}\cdot(\mathbf{r}_C-\mathbf{r}_F)]+\cos[\mathbf{Q}\cdot(\mathbf{r}_D-\mathbf{r}_F)]$
$\cos^2(\alpha/2)\mathcal{L}(\gamma_1+\gamma_2-X,\omega)$ $+\sin^2(\alpha/2)\mathcal{L}(\gamma_1+\gamma_2+X,\omega)$	$\frac{1}{2}\sigma_f$	$2-\cos[\mathbf{Q}\cdot(\mathbf{r}_A-\mathbf{r}_B)]-\cos[\mathbf{Q}\cdot(\mathbf{r}_E-\mathbf{r}_F)]$
$\mathcal{L}(2\gamma_1,\omega)$	$\frac{1}{2}\sigma_s$	$1-\cos[\mathbf{Q}\cdot(\mathbf{r}_C-\mathbf{r}_D)]$

$v_s(q)e^{\imath(2\pi/4)(j-1)(l-1)}$, where the index $j\in\{1,2,3,4\}$ labels the positions of unit cells, $s\in\{1,2\}$ labels the two atomic positions in a unit cell, $(2\pi/4)(l-1)$ is a ''reciprocal lattice vector'' q, and $[v_1(q),v_2(q)]^\top$ are obtained by diagonalizing the ''dynamical matrix:''

$$G(q)_{ss'}=\begin{pmatrix}-(\gamma_1+\gamma_2) & \gamma_1+\gamma_2e^{-\imath q}\\ \gamma_1+\gamma_2e^{+\imath q} & -(\gamma_1+\gamma_2)\end{pmatrix}. \tag{B2}$$

This way one can show that $\mathbf{M}=\mathbf{S}\mathbf{\Lambda}\mathbf{S}^{-1}$, where $\mathbf{\Lambda}$ is the diagonal matrix:

$$\mathbf{\Lambda}=\mathrm{Diag}[0,-2(\gamma_1+\gamma_2),-(\gamma_1+\gamma_2)+1,-(\gamma_1+\gamma_2)-1,$$
$$-2\gamma_1,-2\gamma_2,-(\gamma_1+\gamma_2)+1,-(\gamma_1+\gamma_2)-1] \tag{B3}$$

and

$$\mathbf{S}=\frac{1}{\sqrt{8}}\begin{pmatrix}
1 & +1 & 1 & 1 & +1 & +1 & 1 & 1\\
1 & -1 & \gamma_1+\imath\gamma_2 & -\gamma_1-\imath\gamma_2 & -1 & +1 & \gamma_1-\imath\gamma_2 & -\gamma_1+\imath\gamma_2\\
1 & +1 & \imath & \imath & -1 & -1 & -\imath & -\imath\\
1 & -1 & -\gamma_2+\imath\gamma_1 & \gamma_2-\imath\gamma_1 & +1 & -1 & -\gamma_2-\imath\gamma_1 & \gamma_2+\imath\gamma_1\\
1 & +1 & -1 & -1 & +1 & +1 & -1 & -1\\
1 & -1 & -\gamma_1-\imath\gamma_2 & \gamma_1+\imath\gamma_2 & -1 & +1 & -\gamma_1+\imath\gamma_2 & \gamma_1-\imath\gamma_2\\
1 & +1 & -\imath & -\imath & -1 & -1 & \imath & \imath\\
1 & -1 & \gamma_2-\imath\gamma_1 & -\gamma_2+\imath\gamma_1 & +1 & -1 & \gamma_2+\imath\gamma_1 & -\gamma_2-\imath\gamma_1
\end{pmatrix}. \tag{B4}$$

Furthermore, $\mathbf{S}^{-1}=\mathbf{S}^\dagger$. The Fourier transforms of the configurations XYZ are defined as

$$\mathcal{F}_{XYZ}=b_f e^{\imath\mathbf{Q}\cdot\mathbf{r}_X}+b_s e^{\imath\mathbf{Q}\cdot\mathbf{r}_Y}+b_f e^{\imath\mathbf{Q}\cdot\mathbf{r}_Z}, \tag{B5}$$

where b_f is the scattering length of the rapidly hopping atom (in A, B, E or F), and b_s the scattering length of the slowly hopping atom (in C or D). Defining the row matrix $\mathbb{F}$,

$$\mathbb{F}=[\mathcal{F}_{BCF},\mathcal{F}_{BDF},\mathcal{F}_{ADF},\mathcal{F}_{ACF},\mathcal{F}_{ACE},\mathcal{F}_{ADE},\mathcal{F}_{BDE},\mathcal{F}_{BCE}], \tag{B6}$$

the structure factor can then expressed as $\frac{1}{8}\mathbb{F}\mathbf{S}\mathbb{L}(\omega)\mathbf{S}^\dagger\mathbb{F}^\dagger$, where $\mathbb{L}(\omega)$ is the diagonal matrix containing the normalized to 1 Lorentzians $\mathcal{L}(\omega,\lambda_j)$ of width λ_j where λ_j is taken from $\mathbf{\Lambda}$. By convention a Lorentzian of width 0 is considered to be $\delta(\omega)$. The algebra of the evaluation of this expression is truly considerable and uninspiring. The final result is listed in Table III.

APPENDIX C: CALCULATION FOR SIMULTANEOUS JUMPS

Equation (6) follows from

$$S(\mathbf{Q},\omega)=\sigma\mathbb{F}\frac{1}{\sqrt{2}}\begin{pmatrix}1 & 1\\ 1 & -1\end{pmatrix}\begin{pmatrix}\delta(\omega) & 0\\ 0 & \Lambda(\omega)\end{pmatrix}\times\begin{pmatrix}1 & 1\\ 1 & -1\end{pmatrix}\frac{1}{\sqrt{2}}\mathbb{F}^{\dagger}, \tag{C1}$$

where now

$$\mathbb{F}=[e^{\imath\mathbf{Q}\cdot\mathbf{r}_A}+e^{\imath\mathbf{Q}\cdot\mathbf{r}_C},e^{\imath\mathbf{Q}\cdot\mathbf{r}_B}+e^{\imath\mathbf{Q}\cdot\mathbf{r}_D}]. \tag{C2}$$

APPENDIX D: UNALTERED SITE OCCUPATIONS REMAIN MUTE IN COHERENT MODELS

Let us just consider a system that can swap by an atomic jump between two (energetically equivalent) configurations. The jump matrix will then be the same as the one that leads to Eq. (1). After applying the same sorts of algebra as for this model, the structure factor will read

$$\frac{1}{4}[S_{1,1}(\mathbf{Q})+S_{2,2}(\mathbf{Q})-2S_{1,2}(\mathbf{Q})]\Lambda(\Gamma,\omega)+\frac{1}{4}[S_{1,1}(\mathbf{Q})+S_{2,2}(\mathbf{Q})+2S_{1,2}(\mathbf{Q})]\delta(\omega). \tag{D1}$$

where $\Gamma=4\pi/\tau$ and we have introduced the notation

$$S_{m,n}(\mathbf{Q})=\frac{1}{2}[F_m(\mathbf{Q})F_n^*(\mathbf{Q})+F_n(\mathbf{Q})F_m^*(\mathbf{Q})]. \tag{D2}$$

Here $\mathcal{F}_m(\mathbf{Q})$ is the Fourier transform of configuration j. The quasielastic structure factor can be rewritten as

$$\frac{1}{4}[\mathcal{F}_1(\mathbf{Q})-\mathcal{F}_2(\mathbf{Q})][\mathcal{F}_1(\mathbf{Q})-\mathcal{F}_2(\mathbf{Q})]^*, \tag{D3}$$

and in this expression all contributions from unaltered site occupations cancel.

*Corresponding author. Present address: Laboratoire des Solides Irradiés, Ecole Polytechnique, F-91128-Palaiseau CEDEX, France. Electronic address: Gerrit.Coddens@polytechnique.fr

†Present address: Département de Chimie Moléculaire, C.E.A. Saclay, F-91191-Gif-sur-Yvette CEDEX, France.

[1] G. Coddens, Ann. Chim. (Paris) **18**, 513 (1993); G. Coddens, R. Bellissent, Y. Calvayrac, and J. P. Ambroise, Europhys. Lett. **16**, 271 (1991); G. Coddens, C. Soustelle, R. Bellissent, and Y. Calvayrac, *ibid.* **23**, 33 (1993).

[2] G. Coddens, S. Lyonnard, B. Sepiol, and Y. Calvayrac, J. Phys. I **5**, 771 (1995).

[3] J. H. de Araújo, A. A. Gomes, and J. B. M. da Cunha, Solid State Commun. **97**, 1025 (1996).

[4] R. A. Brand, J. Voss, and Y. Calvayrac, in *Mössbauer Spectroscopy in Materials Science*, Proceedings of the NATO Advanced Workshop, Senec, Slovakia, 1998, edited by M. Miglierini and D. Petridis (Kluwer, Dordrecht, 1999), p. 299.

[5] G. Coddens, S. Lyonnard, and Y. Calvayrac, Phys. Rev. Lett. **78**, 4209 (1997).

[6] S. Lyonnard, G. Coddens, Y. Calvayrac, and D. Gratias, Phys. Rev. B **53**, 3150 (1996).

[7] S. Lyonnard, G. Coddens, B. Hennion, R. Bellissent, and Y. Calvayrac, Physica B **219&220**, 342 (1996); J. Non-Cryst. Solids **205-207**, 11 (1996).

[8] G. Coddens and W. Steurer, Phys. Rev. B **60**, 270 (1999).

[9] Phason hopping has also been observed in computer simulations [M. Hohl, G. Zeger, and R. Trebin (private communication)].

[10] An interesting observation of very-long-time phason correlations is reported by S. Matsuo, T. Ishimasa, and H. Nakano, Solid State Commun. **102**, 575 (1997); S. Matsuo, H. Nakano, and T. Ishimasa, in *Proceedings of the 6th International Conference on Quasicrystals, Yamada Conference XVVII, Tokyo, Japan, 1997*, edited by S. Takeuchi and T. Fujiwara (World Scientific, Singapore, 1998), p. 467. It is to be understood within the framework of the theory of Toner (Ref. 11).

[11] J. Toner, Phys. Rev. B **37**, 9571 (1988).

[12] P. Bak, Phys. Rev. Lett. **54**, 1517 (1985); Phys. Rev. B **32**, 5764 (1985).

[13] T. C. Lubensky, S. Ramaswamy, and J. Toner, Phys. Rev. B **32**, 7444 (1985).

[14] D. M. Frenkel, C. L. Henley, and E. D. Siggia, Phys. Rev. B **34**, 3649 (1986); L. S. Levitov, in *Quasicrystals, The State of the Art*, edited by D. P. diVincenzo and P. J. Steinhardt, *Directions in Condensed Matter Physics*, Vol. 11 (World Scientific, Singapore, 1991), p. 239; A. Katz, in *Proceedings of the Anniversary Adriatico Conference on Quasicrystals, ICTP, Trieste, Italy, 1989*, edited by M. V. Jarić and S. Lundqvist (World Scientific, Singapore, 1989), p. 200; in *Proceedings of the Workshop ''Number Theory in Physics,'' Les Houches, France, 1989*, edited by J. M. Luck, P. Moussa, M. Waldschmidt, and C. Itzykson, *Springer Proceedings in Physics*, Vol. 47 (Springer, Berlin, 1990), p. 100. See, however, also Ref. 15.

[15] For examples of QCs with continuous phasons, see, e.g., P. Kalugin and L. S. Levitov, Int. J. Mod. Phys. B **3**, 877 (1989); M. Wirth and H.-R. Trebin, Europhys. Lett. **13**, 61 (1990). These counterexamples jeopardize the possibility of defining QCs unambiguously on the basis of the nature of the phasons.

[16] P. A. Kalugin, A. Y. Kitaev, and L. Levitov, JETP Lett. **41**, 145 (1985); A. Katz and M. Duneau, Phys. Rev. Lett. **54**, 2688 (1985); J. Phys. (Paris) **47**, 181 (1985); V. Elser, Acta Crystallogr., Sect. A: Found. Crystallogr. **42**, 37 (1986).

[17] R. Currat and T. Janssen, Solid State Phys. **41**, 201 (1988).

[18] The pioneering papers on the random-tiling model are M. Widom, D. P. Deng, and C. L. Henley, Phys. Rev. Lett. **63**, 310 (1989); K. Strandburg, L.-H. Tang, and M. V. Jarić, *ibid.* **63**, 314 (1989). Since then, a vast amount of literature on this topic has been published. It is beyond the concern of this paper to provide the reader here with a comprehensive bibliography on this fascinating chapter of statistical physics.

[19] A. Katz and D. Gratias, J. Non-Cryst. Solids **153&154**, 187 (1993); A. Le Lann and J. Devaud, J. Phys. I **5**, 129 (1995); M. Cornier-Quiquandon, A. Quivy, S. Lefebvre, E. Elkaim, G. Heger, A. Katz, and D. Gratias, Phys. Rev. B **44**, 2071 (1991).

[20] P. A. Kalugin and A. Katz, Europhys. Lett. **21**, 921 (1993).

[21] S. Dworkin and J. I. Shieh, Commun. Math. Phys. **168**, 337 (1995). The model of Kalugin and Katz stands as far as its initial motivation to explain perfect growth is concerned. But it may have taken the argument one step too far in postulating the existence of fast diffusion. It is indeed superfluous to have recourse to long-range diffusion in order to comply with perfect growth. It just suffices to execute a few phason moves in an (ever recurring) *local* canonical environment. The name ''clus-

ter'' has been promoted for this recurrent structural motive [P. Gummelt, Geom. Dedicata **62**, 1 (1996); in *Proceedings of the 6th International Conference on Quasicrystals, Yamada Conference XVVII, Tokyo, Japan, 1997*, edited by S. Takeuchi and T. Fujiwara (World Scientific, Singapore, 1998), p. 148; H.-C. Jeong and P. J. Steinhardt, Phys. Rev. B **55**, 3520 (1997); Nature (London) **382**, 433 (1996)]. Two (''clustrophobic'') *caveats* are due here, as the meaning of such ''clusters'' tends to be overrated in the literature: (1) There is no compelling basis for the doctrine that such ''clusters'' could shed light on the stability of QCs. (2) The covering is just the Penrose tiling with fat and skinny rhombi in a different but isomorphic guise. Any attempt to metamorphose the ''clusters'' into seeds of growth algorithms will thus be wreaked with the very same havoc as previous stratagems that tried to capitalize on the matching rules.

[22] S. W. Kycia, A. I. Goldman, T. A. Lograsso, D. W. Delancy, M. Sutton, E. Dufresne, R. Brüning, and B. Rodrickx, Phys. Rev. B **48**, 3544 (1993).

[23] D. Joseph and V. Elser, Phys. Rev. Lett. **79**, 1066 (1997). This model has been discussed by P. A. Kalugin (unpublished).

[24] A strongly akin idea of a phason-related phase transition appears in other publications, which we cite here and under the next two reference citations. Within the framework of the random-tiling model: C. L. Henley, *Quasicrystals, The State of the Art* (World Scientific, Singapore, 1991) p. 429; L.-H. Tang and M. V. Jarić, Phys. Rev. B **41**, 4524 (1990); H. C. Jeong and P. J. Steinhardt (unpublished); W. Ebinger, J. Roth, and H. R. Trebin, Phys. Rev. B **58**, 8338 (1998).

[25] Within an Ising model context: T. Dotera and P. J. Steinhardt, Phys. Rev. Lett. **72**, 1670 (1994); H. C. Jeong and P. J. Steinhardt, Phys. Rev. B **48**, 9394 (1994); T. Dotera, Mater. Sci. Eng., A **181&182**, 758 (1994); Mater. Sci. Forum **150&151**, 375 (1994).

[26] Within the framework of a diffusion model: F. Gähler, in *Proceedings of the Fifth International Conference on Quasicrystals, Avignon, France, 1995*, edited by C. Janot and R. Mosseri (World Scientific, Singapore, 1996), p. 236.

[27] A. Trub and H.-R. Trebin, J. Phys. I **4**, 1855 (1994); D. Joseph, M. Baake, P. Kramer, and H.-R. Trebin, Europhys. Lett. **27**, 451 (1994); A. Rüdinger and H.-R. Trebin, J. Phys. A **27**, 7981 (1994).

[28] M. V. Jarić and E. S. Sørensen, Phys. Rev. Lett. **73**, 2464 (1994).

[29] F. Gähler and J. Roth, in *Proceedings of the International Conference on Aperiodic Crystals, Les Diablerets, Switzerland, 1994*, edited by G. Chapuis and W. Paciorek (World Scientific, Singapore, 1995), p. 183; D. Joseph and F. Gähler, *ibid.*, p. 188; F. Gähler and A. Hirning (unpublished).

[30] M. Dzugutov, Europhys. Lett. **31**, 95 (1995).

[31] ^{59}Fe in Al-Cu-Fe: J.-L. Joulaud, C. Bergman, J. Bernardini, P. Gas, J.-M. Dubois, Y. Calvayrac, and D. Gratias, J. Phys. IV **6**, 259 (1996); J. L. Joulaud, J. Bernardini, P. Gas, C. Bergman, J. M. Dubois, Y. Calvayrac, and D. Gratias, Philos. Mag. A **75**, 1287 (1997).

[32] ^{54}Mn and ^{59}Fe in Al-Mn-Pd: Th. Zumkley, H. Mehrer, K. Freitag, M. Wollgarten, N. Tamura, and K. Urban, Phys. Rev. B **54**, R6815 (1996); T. Zumkley, M. Wollgarten, M. Feuerbacher, K. Freitag, and H. Mehrer, Defect Diffus. Forum **143-147**, 843 (1997).

[33] ^{54}Mn in Al-Mn-Pd: W. Sprengel, T. A. Lograsso, and H. Nakajima, Phys. Rev. Lett. **77**, 5233 (1996); H. Nakajima, J. Asai, K. Nonaka, I. Shinbo, A. Tsai, and T. Matsumoto, Mater. Sci. Eng., A **181/182**, 738 (1994); H. Nakajima, J. Asai, N. Nonaka, I. Shinbo, A. Tsai, and T. Matsumoto, Philos. Mag. Lett. **68**, 315 (1993).

[34] ^{54}Mn and ^{68}Ge in Al-Mn-Pd: W. Sprengel, T. A. Lograsso, and H. Nakajima, Defect Diffus. Forum **143-147**, 849 (1997); H. Nakajima, W. Sprengel, and K. Nonaka, *ibid.* **143-147**, 803 (1997).

[35] ^{60}Co in Al-Mn-Pd: W. Sprengel, H. Nakajima, and T. A. Lograsso, in *Proceedings of the 6th International Conference on Quasicrystals, Yamada Conference XVVII, Tokyo, Japan, 1997*, edited by S. Takeuchi and T. Fujiwara (World Scientific, Singapore, 1998), p. 429.

[36] ^{24}Na and ^{59}Co in Al-Cu-Fe: V. I. Franchouk and L. N. Larikov, Defect Diffus. Forum **143-147**, 855 (1997).

[37] ^{103}Pd and ^{195}Au in Al-Mn-Pd: R. Blüher, P. Scharwaechter, W. Frank, and H. Kronmüller, Phys. Rev. Lett. **80**, 1014 (1998).

[38] V. Elser, Philos. Mag. A **73**, 641 (1996); in *Proceedings of the 6th International Conference on Quasicrystals, Yamada Conference XVVII, Tokyo, Japan, 1997*, edited by S. Takeuchi and T. Fujiwara (World Scientific, Singapore, 1998), p. 19.

[39] P. Kramer, Z. Papadopolos, and W. Liebermeister, in *Proceedings of the 6th International Conference on Quasicrystals, Yamada Conference XVVII, Tokyo, Japan, 1997*, edited by S. Takeuchi and T. Fujiwara (World Scientific, Singapore, 1998), p. 71.

[40] G. Coddens and P. Launois, J. Phys. I **1**, 993 (1991); R. Mosseri, J. Non-Cryst. Solids **153&154**, 658 (1993).

[41] See, e.g., P. A. Bancel, in *Quasicrystals, The State of the Art*, edited by D. P. DiVincenzo and P. J. Steinhardt, *Directions in Condensed Matter Physics*, Vol. 11 (World Scientific, Singapore, 1991), p. 17.

[42] W. Steurer, M. Honal, and T. Haibach, in *Proceedings of the 6th International Conference on Quasicrystals, Yamada Conference XVVII, Tokyo, Japan, 1997*, edited by S. Takeuchi and T. Fujiwara (World Scientific, Singapore, 1998), p. 355; M. Honal, T. Haibach, and W. Steurer, Acta Crystallogr., Sect. A: Found. Crystallogr. **54**, 374 (1998).

[43] L. Beraha, M. Duneau, H. Klein, and M. Audier, Philos. Mag. A **A76**, 587 (1997); **78**, 345 (1998); L. Beraha, M. Duneau H. Klein, and M. Audier, in *Proceedings of the 6th International Conference on Quasicrystals, Yamada Conference XVVII, Tokyo, Japan, 1997*, edited by S. Takeuchi and T. Fujiwara (World Scientific, Singapore, 1998), pp. 207 and 363; H. Klein, M. Audier, M. Boudard, M. de Boissieu, L. Beraha, and M. Duneau, Philos. Mag. A **73**, 309 (1996); H. Klein, M. Boudard, M. de Boissieu, M. Audier, H. Vincent, L. Beraha, and M. Duneau, *ibid.* **75**, 197 (1997). These results represent the first structural confirmation of the existence of phason jumps. The jump distances observed are comparable with ours.

[44] L. Bresson, in *Lectures on Quasicrystals*, edited by F. Hippert and D. Gratias (Les Editions de Physique, Les Ulis, 1994), p. 549; L. Bresson, A. Quivy, F. Faudot, M. Quiquandon, and Y. Calvayrac, in *Proceedings of the 6th International Conference on Quasicrystals, Yamada Conference XVVII, Tokyo, Japan, 1997*, edited by S. Takeuchi and T. Fujiwara (World Scientific, Singapore, 1998), p. 211; M. Feuerbacher, M. Bartsch, B. Grushko, U. Messerschmidt, and K. Urban, Philos. Mag. Lett. **76**, 369 (1997).

[45] T. Dotera, in *Proceedings of the 6th International Conference on Quasicrystals, Yamada Conference XVVII, Tokyo, Japan, 1997*,

edited by S. Takeuchi and T. Fujiwara (World Scientific, Singapore, 1998), p. 501.

[46] M. Feuerbacher, M. Weller, J. Diehl, and K. Urban, Philos. Mag. Lett. **74**, 81 (1996), reported internal-friction data obtained by vibrating-reed experiments, which they interpreted in terms of phason dynamics. They found activation enthalpies of 0.98 eV (at low temperatures) and 4.0 eV (at high temperatures) in $Al_{72.1}Mn_{7.2}Pd_{20.7}$. See also M. Feuerbacher, M. Weller, and K. Urban, in *Proceedings of the 6th International Conference on Quasicrystals, Yamada Conference XVVII, Tokyo, Japan, 1997*, edited by S. Takeuchi and T. Fujiwara (World Scientific, Singapore, 1998), p. 521.

[47] S. Lyonnard, Ph.D. thesis, Orsay University, 1997.

[48] E. A. Hill, T. C. Chang, Y. Wu, S. J. Poon, F. S. Pierce, and Z. M. Stadnik, Phys. Rev. B **49**, 8615 (1994). In the analysis presented by these authors it has been assumed that $\omega_0\tau_c \gg 1$. Here ω_0 is the NMR frequency. If the relaxation time $\tau_c = \hbar/\Gamma$ is characteristic of atomic hopping, one should have $\omega_0\tau_c \ll 1$, since the hopping is very fast. In the series expansion $M(\tau) = M(\tau_\infty) \times [\Sigma_j e^{-c_j W_1 \tau}]$, used in the reference, the term $W_1 = \alpha\tau_c/[1 + (\omega_0\tau_c)^2]$, where $\tau_c(T) = \tau_c(\infty)e^{E_a/kT}$, corresponds to a Lorentzian $W_1 = \alpha\hbar\Gamma/[\Gamma^2 + (\hbar\omega_0)^2]$. In the high-temperature limit it becomes $W_1 = \alpha\tau_c$ and $W_1(T) = W_1(\infty)e^{E_a/kT}$, while the low-temperature limit corresponds to $W_1(T) = W_1(\infty)e^{-E_a/kT}$. In both limiting cases one will find an Arrhenius law, but with a different sign in the Boltzmann factor. The temperature dependence of the data, which implies that W increases with increasing temperature, seems to be compatible only with $W_1(T) = W_1(\infty)e^{-E_a/kT}$ and makes the conclusion $\omega_0\tau_c \gg 1$ inevitable. But the neutron-scattering experiments show that the width of the Lorentzian signal practically does not change with temperature, and that it is the intensity that follows an Arrhenius plot. Hence the NMR data can nevertheless be in the high-temperature limit, if we assume that in $W_1 = \alpha\tau_c$, it is the intensity prefactor α that is responsible for the Arrhenius behavior of W_1 instead of τ_c. A detailed study of this problem is on its way [D. Massiot, F. Hippert, V. Simonet, and G. Coddens (private communication)].

[49] J. Dolinšek, B. Ambrosini, P. Vonlanthen, J. L. Gavilano, M. A. Chernikov, and H. R. Ott, Phys. Rev. Lett. **81**, 3671 (1998).

[50] L. Van Hove, Phys. Rev. **51**, 249 (1954); W. Marshall and S. Lovesey, *Theory of Neutron Scattering from Condensed Matter*, (Clarendon Press, Oxford, 1984).

[51] M. Bée, *Quasielastic Neutron Scattering* (Adam Hilger, Bristol, 1988).

[52] T. Springer, *Quasielastic Neutron Scattering, Springer Tracts in Physics*, Vol. 64 (Springer-Verlag, Berlin, 1972).

[53] R. E. Lechner, in *Proceedings of the Conference on Neutron Scattering, Gatlinburg, 1976*, edited by R. M. Moon (National Technical Information Service, U.S. Department of Commerce, Springfield, 1976), Vol. 1, p. 310.

[54] A. P. Tsai, A. Inoue, and T. Matsumoto, Jpn. J. Appl. Phys., Part 2 **26**, L1505 (1987).

[55] A. P. Tsai, A. Inoue, Y. Yokoyama, and T. Matsumoto, Philos. Mag. Lett. **61**, 9 (1990); Y. Yokoyama, T. Miura, A. P. Tsai, A. Inoue, and T. Masumoto, Mater. Trans., JIM **33**, 97 (1992).

[56] T. A. Lograsso and D. W. Delaney, in *Proceedings of the 6th International Conference on Quasicrystals, Yamada Conference XVVII, Tokyo, Japan, 1997*, edited by S. Takeuchi and T. Fujiwara (World Scientific, Singapore, 1998), p. 325.

[57] T. J. Sato, T. Hirano, and A. P. Tsai, in *Aperiodic '97*, Proceedings of the International Conference on Aperiodic Crystals, Alpe d'Huez, France, 1997, edited by M. de Boissieu, J.-L. Vergy-Gaugry, and R. Currat (World Scientific, Singapore, 1988), p. 523; J. Cryst. Growth **191**, 545 (1998).

[58] I. R. Fisher, M. J. Kramer, Z. Islam, A. R. Ross, A. Kracher, T. Wiener, M. J. Sailer, A. I. Goldman, and P. C. Canfield, Philos. Mag. B **79**, 425 (1999).

[59] It is important to use samples that are as perfect as possible. In imperfect samples additional dynamics may show up, which are delicate to interpret. See, e.g., K. Shibata, H. Mizuseki, A. P. Tsai, and K. Suzuki, Physica B **213&214**, 573 (1995).

[60] The most sensational example probably being the determination of the structure of the ribozome by small-angle neutron scattering. See, e.g., V. Ramakrishnan, Physica B **136**, 232 (1986).

[61] S. F. Mughabghab, M. Divadeenam, and N. E. Holden, *Neutron Cross Sections* (Academic Press, New York, 1981).

[62] M. Quiquandon, A. Quivy, F. Faudot, N. Sâadi, Y. Calvayrac, S. Lefebvre, and M. Bessière, in *Proceedings of the Fifth International Conference on Quasicrystals, Avignon, France, 1995*, edited by C. Janot and R. Mosseri (World Scientific, Singapore, 1996), p. 154.

[63] T. Gödecke and R. Lück, Z. Metallkd. **86**, 109 (1995).

[64] E. Gerdau, R. Rüffer, R. Hollatz, and J.P. Hannon, Phys. Rev. Lett. **57**, 1141 (1986).

[65] C. Janot, A. Magerl, B. Frick, and M. de Boissieu, Phys. Rev. Lett. **71**, 871 (1993), missed the quasielastic neutron-scattering and Mössbauer-spectroscopy signals of Fe hopping reported in Refs. 2, 4, and 5, but they did observe the corresponding *elastic* effect in the temperature dependence of the Debye-Waller factor. As the quasielastic counterpart was not seen, the temperature dependence of the Debye-Waller factor looked anomalous. The authors interpreted this in terms of localized modes on clusters and they suggested that our data should be reinterpreted along the same lines. Our opinion about these suggestions has been laid down in Refs. 5 and 6. Within the domain of Mössbauer spectroscopy our hopping interpretation has been validated by three independent results (Refs. 2–4).

[66] J.-M. Dubois (unpublished) has suggested that the quasielastic signal should be reinterpreted within the framework of a structural model of M. de Boissieu, P. Stephens, M. Boudard, C. Janot, D. L. Chapman, and M. Audier, J. Phys.: Condens. Matter. **61**, 7251 (1994) in terms of rotating clusters (molecules). Our opinion about these suggestions is Ref. 6. The underlying ''cluster'' picture has been further criticized by C. L. Henley, in *Proceedings of the 6th International Conference on Quasicrystals, Yamada Conference XVVII, Tokyo, Japan, 1997*, edited by S. Takeuchi and T. Fujiwara (World Scientific, Singapore, 1998), p. 27.

[67] M. de Boissieu, M. Boudard, S. Kycia, A. I. Goldman, B. Hennion, R. Bellissent, M. Quilichini, R. Currat, and C. Janot, in *Proceedings of the Fifth International Conference on Quasicrystals, Avignon, France, 1995*, edited by C. Janot and R. Mosseri (World Scientific, Singapore, 1996), p. 577. These authors have suggested an alternative interpretation of the quasielastic signal in terms of ''long-wavelength phason fluctuations.'' Our opinion about these suggestions has been voiced in Ref. 74. See also Refs. 14.

[68] J.-M. Dubois, in *Proceedings of the 6th International Conference on Quasicrystals, Yamada Conference XVVII, Tokyo, Japan, 1997*, edited by S. Takeuchi and T. Fujiwara (World Scientific, Singapore, 1998), p. 785; U. Dahlborg, M. Calvo-Dahlborg,

J.-M. Dubois, and W. S. Howells (unpublished). These authors claim that fast atomic jumps are nothing special for QCs. Our opinion about these claims is given in Appendix A.

[69] C. Janot and J.-M. Dubois, *Les Quasicristaux, Matière à Paradoxes* (Editions de Physique, Les Ulis, 1998). These authors state that the quasielastic signal is *minuscule* and that its existence can only be established *numerically* with the aid of a fit program. The reader can check if this is true in the figures of the present paper.

[70] G. Coddens, A. M. Viano, P. C. Gibbons, K. F. Kelton, and M. J. Kramer, Solid State Commun. **104**, 179 (1997).

[71] G. Coddens, A. M. Viano, P. C. Gibbons, K. F. Kelton, M. J. Kramer, J. Tomkison, and H. Casalta (unpublished).

[72] G. Coddens, Int. J. Mod. Phys. B **7**, 1679 (1997).

[73] M. de Boissieu, M. Boudard, A. Letoublon, B. Frick, and C. Janot (unpublished); M. Boudard, M. de Boissieu, A. Letoublon, B. Hennion, R. Bellissent, and C. Janot, Europhys. Lett. **33**, 199 (1996); M. de Boissieu, M. Boudard, S. Kycia, A. I. Goldman, B. Hennion, R. Bellissent, M. Quilichini, R. Currat, and C. Janot, in *Proceedings of the Fifth International Conference on Quasicrystals, Avignon, France, 1995*, edited by C. Janot and R. Mosseri (World Scientific, Singapore, 1996), p. 577; (unpublished).

[74] A very different approach to phason dynamics has been developed by Ishii [Y. Ishii, in *Proceedings of the 5th International Conference of Quasicrystals, Avignon, France, 1995*, edited by C. Janot and R. Mosseri (World scientific, Singapore, 1996), p. 359; in *Proceedings of the 6th International Conference on Quasicrystals, Yamada Conference XVVII, Tokyo, Japan, 1997*, edited by S. Takeuchi and T. Fujiwara (World Scientific, Singapore, 1998), p. 459]. However, this approach is more related to the very-long-time behavior as reported in Ref. 10.

[75] G. Coddens and S. Lyonnard, Physica B **226**, 28 (1996); **233**, 93 (1997).

[76] R. Caudron, A. Finel, Y. Calvayrac, M. Fradkin, and R. Bellissent, in *Proceedings of the 6th International Conference on Quasicrystals, Yamada Conference XVVII, Tokyo, Japan, 1997*, edited by S. Takeuchi and T. Fujiwara (World Scientific, Singapore, 1998), p. 375.

[77] F. Hippert (private communication).

[78] L. Pintschovius, Nucl. Instrum. Methods Phys. Res. A **338**, 136 (1994).

[79] M. J. Cooper and R. Nathans, Acta Crystallogr. **23**, 357 (1967); Acta Crystallogr., Sect. A: Cryst. Phys., Diffr., Theor. Gen. Crystallogr. **24**, 481 (1968).

[80] B. De Raedt and K. H. Michel, Phys. Rev. B **19**, 767 (1979); K. H. Michel and J. Naudts, J. Chem. Phys. **68**, 216 (1978).

[81] C. Huygens, *Horologium Oscillatorium* (North-Holland, Amsterdam, 1673).

[82] G. Zeger and H. R. Trebin, Phys. Rev. B **54**, R720 (1996); D. Wofangel, M.D. thesis, Stuttgart University, 1998).

[83] G. Coddens, J. Phys. I **4**, 921 (1994).

[84] S. Aubry and G. André, in *The Physics of Quasicrystals*, edited by P. Steinhardt and S. Ostlundt (World Scientific, Singapore, 1987), p. 554.

[85] T. Janssen (private communication).

[86] H. R. Trebin (private communication).

[87] M. J. Capitán, Y. Calvayrac, J. L. Joulaud, and D. Gratias (private communication).

[88] In order to validate the interpretation of the quasielastic signal in terms of atomic hopping (as has been urged in Refs. 65–67, and 69), it would have been quite instrumental to make isotopic-contrast studies, as we pointed out in Sec. III. In this respect it is a pity that the authors used the ''zero compound'' of Ni, which has a zero *coherent* scattering cross section, but a strong *total* scattering cross section. We have pointed out in the past that the quasielastic scattering follows the *total* scattering cross sections. The isotopic contrast between ^{0}Ni and ^{nat}Ni is thus not the strongest one could get within the Ni system. Moreover, the Ni accounts only for 15 at. % of the sample, while Cu accounts for 35 at. %. The contrast could have been strongly enhanced by using their ^{65}Cu-enriched sample.

[89] The statement of Y. Yan, S. J. Pennycook, and A. P. Tsai, Phys. Rev. Lett. **81**, 5145 (1998), that they would have provided direct evidence for the presence of vacancies in a decagonal Al-Co-Ni quasicrystal, should not be taken too literally as it is based on a misconception of the definition of a vacancy. In fact, they observe pairs of atomic columns that are too close to be fully occupied simultaneously. Of the two adjacent sites these columns define in a plane, only one can be occupied at the time, since there is simply not enough space available to accomodate two atoms. An unoccupied site of this type cannot be called a vacancy if its twin site is occupied. An analogous situation occurs within the elementary octagon of an eightfold Penrose-like tiling with fat and skinny rhombi. Inside the basic octagon of this tiling we always find three vertices of the tiling. If the vertices are atomic positions, then there are eight different ways to orient these atomic triads within the interior of the octagon: They can be generated one from another by phason moves (as illustrated in the figures of Refs. 20 and 83). The three atoms can visit in total eight positions which trace a smaller, *virtual* octagon inside the initial octagon. One could thus loosely say that these eight interior ''sites'' have an occupation of 3/8, but this does not imply that there would be a 5/8 vacancy concentration, as the five ''remaining sites'' are a pure product of our imagination, and have no physical reality: They cannot possibly be filled with atoms. In fact, there are no vacancies at all in this perfect octagonal tiling, and the situation is better described by saying that there are three real sites and five virtual sites.

[90] L. Mancini, E. Reiner, P. Cloetens, J. Gastaldi, J. Härtwig, M. Schlenker, and J. Baruchel, Philos. Mag. A **78**, 1175 (1998). The presence of these large voids rather tends to suggest that they are sinks for the thermal vacancies, such that these are apparently not so eager to keep roaming around inside the QCs.

[91] A. J. Bradley and A. Taylor, Proc. R. Soc. London, Ser. A **159**, 56 (1937).

[92] A. G. Balogh, I. Dézsi, J. Pelloth, R. A. Brand, W. Keune, and W. Puff, Mater. Sci. Forum **105-110**, 897 (1992).

[93] X. Yusheng, M. Ghafari, H. Hahn, U. Gonser, and B. Molnar, Solid State Commun. **61**, 779 (1987).

[94] F. Hippert, R. A. Brand, J. Pelloth, and Y. Calvayrac, J. Phys.: Condens. Matter **6**, 11189 (1994).

[95] R. Chidambaram, M. K. Sanyal, P. M. G. Nambissan, and P. Sen, Met., Mater. Processes **8**, 45 (1996); J. Phys.: Condens. Matter **2**, 251 (1990); **2**, 9941 (1990).

[96] M. Kogachi, S. Minamigawa, and K. Nakahigashi, Acta Metall. Mater. **40**, 1113 (1992).